Journal of Ethnopharmacology 337 (2025) 118939

Contents lists available at ScienceDirect

Journal of Ethnopharmacology

journal homepage: www.elsevier.com/locate/jethpharm

WuYou decoction effectively reduces neuronal damage, synaptic dysfunction, and Aβ production in rats exposed to chronic sleep deprivation by modulating the Aβ-related enzymes and SIRT1/Nrf2/NF-κB pathway

Zhengyu Wang [a,1], Dan Wu [a,1], Xinyi Hu [a,1], Xuan Hu [a], Qihang Zhu [a], Bixuan Lai [a], Chuhua Zeng [a,b,**], Qinghua Long [a,c,*]

[a] Health Medical Center, Hubei Minzu University, Enshi, 445000, PR China
[b] School of Basic Medical Sciences, Yunnan University of Chinese Medicine, Kunming, 650500, PR China
[c] Hubei Provincial Key Laboratory of Occurrence and Intervention of Rheumatic Disease, Hubei Minzu University, Enshi, 445000, PR China

ARTICLE INFO

Keywords:
WuYou decoction
Chronic sleep deprivation
Neuronal damage
Synaptic dysfunction
Aβ production
SIRT1/Nrf2/NF-κB pathway

ABSTRACT

Ethnopharmacological relevance: Chronic sleep deprivation (CSD) can result in neuronal damage, synaptic dysfunction, Aβ production, neuroinflammation, and ultimately cognitive deterioration. WuYou Decoction (WYD), a contemporary prescription, has shown promise in enhancing sleep quality and cognitive performance in individuals with insomnia. However, the specific molecular mechanisms responsible for the neuroprotective effects of WYD on CSD remain incompletely understood.

Aim of the study: This study aimed to investigate the neuroprotective effects of WYD on the CSD model and its molecular mechanism.

Materials and methods: UHPLC-MS/MS analysis was utilized to analyze the active ingredients of WYD extract. The study employed the multi-platform water environment method to establish the CSD model in rats. Subsequent to treatment with varying doses of WYD in CSD rats, cognitive function and pathological alterations in hippocampus and cortex, including neuronal damage, synaptic dysfunction, Aβ production, and neuroinflammation, were evaluated through a combination of Morris Water Maze test, HE staining, Nissl staining, Golgi-Cox staining, Transmission electron microscope, ELISA, Immunohistochemistry staining, Immunofluorescence staining and Western blot.

Results: UHPLC-MS/MS analysis revealed a total of 99 active ingredients were identified from the WYD extract. The administration of WYD exhibited a mitigation of cognitive decline in the model of CSD, as evidenced by increased neuron count in the hippocampus and cortex, and improved density and length of dendritic spines in these brain regions. Furthermore, WYD was found to suppress the Aβ production, and inhibit the expression of BACE1, PS1, GFAP, IBA1, IL-1β, IL-6, TNF-α, phosphorylated IκBα (Ser32) and phosphorylated NF-κB p65 (Ser536) in the hippocampus and cortex, while also increasing the levels of PSD95, SYN1, ADAM10, IDE, SIRT1 and Nrf2.

Conclusions: WYD exhibits neuroprotective properties in CSD, potentially through modulation of the Aβ-related enzymes and SIRT1/Nrf2/NF-κB pathway.

1. Introduction

Sufficient sleep is necessary to maintain health and cognitive function. Insomnia can have detrimental impacts on human well-being, increase the likelihood of suffering from Alzheimer's disease (AD) (Morin and Jarrin, 2022; Xiong et al., 2024). Chronic sleep deprivation (CSD) can severely cause psychological and behavioral abnormalities including cognitive decline. Currently, cognitive behavioral therapy is considered as a cost-effective strategy to treat sleep disorder-related cognitive impairment, and therapeutic drugs are still limited (Dopheide, 2020; Paul et al., 2022).

* Corresponding author. Health Medical Center, Hubei Minzu University, Enshi, 445000, PR China.
** Corresponding author. Health Medical Center, Hubei Minzu University, Enshi, 445000, PR China.
E-mail addresses: 16155576@qq.com (C. Zeng), 287201413@qq.com (Q. Long).
[1] These authors contributed equally to this work and shared first authorship.

https://doi.org/10.1016/j.jep.2024.118939
Received 8 September 2024; Received in revised form 10 October 2024; Accepted 12 October 2024
Available online 15 October 2024

Abbreviations

CSD	Chronic sleep deprivation
AD	Alzheimer's disease
CNS	Central Nervous System
WYD	WuYou Decoction
MWM	Morris water maze
UHPLC-MS/MS	Ultra-Performance Liquid Chromatography/Mass Spectrometry
HE	Hematoxylin-eosin
ICH	Immunohistochemistry
ELISA	Enzyme-Linked Immunosorbent Assay
TEM	Transmission electron microscope
NeuN	Neuronal nuclear protein
PSD95	Postsynaptic density protein 95
SYN1	Synapsin I
PSD	Postsynaptic density
Aβ	Amyloid beta
ADAM10	A disintegrin and metalloproteinase 10
BACE1	β-site APP cleaving enzyme 1
PS1	Presenilin 1
IDE	Insulin-degrading enzyme
Aβ1-40	Amyloid peptide1-40
Aβ1-42	Amyloid peptide1-42
IBA1	Ionized calcium-binding adaptor molecule 1
GFAP	Glial fbrillary acidic protein
IL-1β	Interleukin-1β
IL-6	nterleukin-6
TNF-α	Tumor necrosis factor-α
SIRT1	Sirtunin 1
Nrf2	Nuclear factor E2-related factor 2
NF-κB	Nuclear factor-kappa B

WuYou Decoction (WYD), a famous herbal prescription, formulated by Chen Shi-Duo. WYD is composed of 5 herbal medicines, namely, dried root and rhizome of *Panax ginseng* C. A. Mey. (Latin name: Ginseng Radix Et Rhizoma, Chinese name: Renshen), the dried and ripe seeds of *Zizipgus jujuba* Mill. var. spinosa (Bunge) Hu ex H. F. Chou (Latin name: Ziziphi Spinosae Semen, Chinese name: Suanzaoren), dried root of *Angelica sinensis* (Oliv.) Diels (Latin name: Angelicae Sinensis Radix, Chinese name:

Danggui), dried root of *Paeonia lactiflora* Pall. (Latin name: Paeoniae Radix Alba, Chinese name: Baishao) and dried intermediate layer of stem of *Sinocalamus beecheyanus* (Munro) McClure var. *pubescens* P. F. Li (Latin name: Bambusae Caulis in Taenias, Chinese name: Zhuru). According to traditional Chinese medicine theory, sleep disorders are intricately linked to deficiencies in qi and blood, as well as to the obstruction caused by phlegm and heat. The therapeutic approaches for addressing sleep disorders include the tonification of qi and nourishment of blood, alongside the clearance of heat and resolution of phlegm. WYD is purported to possess the properties of nourishing qi and blood, clearing heat, and resolving phlegm, thereby offering potential treatment for sleep disorders and amnesia. After the creation of WYD in the Qing Dynasty, Chinese medicine clinical practitioners have commonly utilized it to address symptoms of insomnia and depression (Qin et al., 2014; Tang, 2014). Research indicates that WYD improves cognitive abilities in insomniac sufferers and mitigates neuronal damage in models of depression through the modulation of neurotransmitters (Li and Qin, 2019; Tang, 2014). Nevertheless, the molecular mechanisms of WYD's effect on cognitive function of CSD remain to be further investigated.

Neuronal damage and synaptic dysfunction act as a major contributor to CSD-induced cognitive impairment. Meanwhile, increasing research confirms that increased amyloid beta (Aβ) production could be found in acute or chronic sleep restriction, and the inhibition Aβ expression can alleviate neuronal damage and synaptic dysfunction in CSD models (Niu et al., 2022; Parhizkar et al., 2023; Zhao et al., 2019). CSD can cause inflammatory reaction in neurons, which in turn leads to impaired neurons and synapses. Neuroinflammation is primarily triggered by the activation of glial cells, specifically astrocytes and microglia. Previous studies (Bellesi et al., 2017; Du et al., 2023; Wadhwa et al., 2017; Zielinski et al., 2014) have demonstrated that during CSD, astrocytes and microglia become activated, which triggers the release of inflammatory molecules. Inflammatory elements may have negative impacts on the development and viability of neurons as well as on synaptic flexibility. Consequently, it is believed that blocking neuroinflammation may be a useful tactic for lessening the neuronal damage and synaptic dysfunction caused by CSD.

Sirtuin 1 (SIRT1) is a sensitive factor of neuroinflammation and oxidative stress. Numerous studies (J. Chen et al., 2023; Y. Li et al., 2023; Yang et al., 2022) have demonstrated that SIRT1 can reduce neuroinflammation, oxidative stress, ferroptosis, and mitochondrial dysfunction through the regulation of downstream regulatory factors like nuclear factor E2-related factor 2 (Nrf2). Sleep deprivation hindered the function of the SIRT1/Nrf2 pathway but activating this pathway could help reduce neuronal damage and synaptic dysfunction in models of CSD, ultimately improving cognitive function. Additionally, Nuclear factor-kappa B (NF-κB) can be inhibited by the activation of the SIRT1/Nrf2 pathway, ultimately decreasing the secretion of inflammatory molecules (T. Gao et al., 2023; Y. J. Li et al., 2023; Lu et al., 2020; Wang et al., 2022). Hence, regulation of the SIRT1/Nrf2/NF-κB. pathway could reduce neuronal damage and synaptic dysfunction in CSD by suppressing neuroinflammation.

The objective of this study is to examine the neuroprotective effects and underlying molecular mechanisms of WYD in ameliorating cognitive deficits, neuronal damage, synaptic dysfunction, and Aβ production induced by CSD via regulating the Aβ-related enzymes and SIRT1/Nrf2/NF-κB pathway.

2. Materials and methods

2.1. Animals and treatments

Fifty male Sprague Dawley rats, weighing 200–220g, and were purchased from Changsheng Biotechnology Co., Ltd. (Liaoning, China; certification number: SCXK (Liaoning) 2020-0001). Rats were housed in the Hubei Provincial Key Laboratory of Occurrence and Intervention of Rheumatic Disease under conditions of 25 °C, a humidity range of 50–60%, a 12-h light-dark cycle, and given unlimited food and water. The Health Ethics Committee of Hubei Minzu University reviewed and authorized the experimental procedures (authorization number: 202382). One week following the implementation of flexible feeding, the rats were randomly allocated into 5 distinct groups, each comprising 10 rats: the Control group, the Model group, the low-dose WYD (L-WYD) group, the medium-dose WYD (M-WYD) group, and the high-dose WYD (H-WYD) group. All groups of rats, excluding the Control group, underwent 21 consecutive days of CSD. During the period of CSD and the subsequent 7 days, encompassing a total duration of 28 days, both the Control and Model groups received an equivalent oral administration of saline solution. Consistent with the principle of clinical equivalent dosing and supported by the prior research (Li and Qin, 2019), the groups treated with WYD received 3 different dosages of WYD extract through intragastric administration (L-WYD: 3.99 g/kg/d, M-WYD: 7.98 g/kg/d, H-WYD: 15.96 g/kg/d) over a period of 28 days. The experimental flowchart and critical stages of the experiment are depicted in

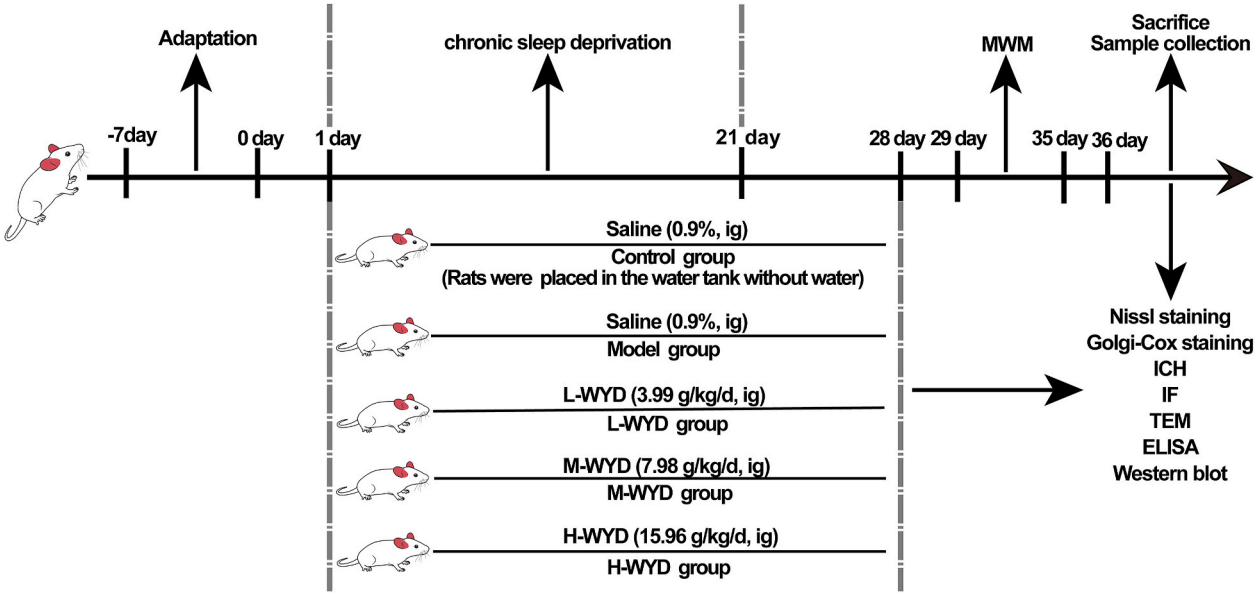

Fig. 1. The experimental flowchart and critical stages in this study.

Fig. 1.

2.2. Establishment of CSD model

The CSD model was created using the multi-platform water environment method, in line with previous research (Kang et al., 2023; Z. H. Li et al., 2022; Lu et al., 2020). Briefly, the sleep deprivation device consists of a water tank and six interconnected cylinders (10 cm in diameter), and the distance between adjacent cylinders is 15 cm. While experiencing sleep deprivation, the water tank was filled up to 1 cm below the top of the cylinder. Following that, rats were positioned inside the circular platforms with unrestricted access to food and water. When rats entered the sleep phase, they fell into the water and woke up, thereby staying awake. In this study, rats in the Model and WYD-treated groups underwent a 21-day period of CSD. Meanwhile, the control group of rats were housed in dry tanks devoid of water.

2.3. Preparation of WYD extract

The drugs of WYD were obtained from Anhui QunKang Pharmaceutical Technology Co., Ltd, and the detailed information about the herbal ingredients of WYD is listed in Table 1. The WYD extract was prepared in accordance with the national pharmacopoeia standard. Briefly, all herbs were immersed in pure water for 30 min (1:8, w/v). Subsequently, the mixed herbs were brought to a boil for 30 min, and then filtered. The residual herbs are mixed again with pure water (1:6, w/v), and boiled for 20 min. The drug solution was collected through filtration. The two drug solutions were mixed, boiled, and concentrated into a stock solution. High doses of WYD were four times and twice as high as low and medium doses, respectively.

2.4. An analysis of the WYD extract using UHPLC-MS/MS

A mixture consisting of 1 mL of WYD solution and 3 mL of ethanol was subjected to sonication for 10 min in an ice bath. Following a 12-h incubation period, the mixture underwent centrifugation to isolate the supernatant. The ethanol present in the supernatant was subsequently evaporated using nitrogen gas. For further analysis, a 10 μL aliquot of the prepared solution was injected into a SHIMADZU-LC30 UHPLC system. Chromatographic separation was achieved using an ACQUITY UPLC® HSS T3 column (2.1 × 100 mm, 1.8 μm). The column temperature was maintained at 40 °C, with a flow rate set at 0.3 mL/min. Each sample was conducted in both positive and negative ion modes utilizing electrospray ionization (ESI). Following UPLC separation, the sample was analyzed using a Thermo Scientific mass spectrometer, with ionization performed via a HESI source. Detailed methodologies for chromatographic separation, mass spectrometry analysis, and data collection are provided in Supplementary 1. The raw mass spectrometry data were processed using MS DIAL software, which encompassed alignment, retention time correction, and peak area extraction. Based on a previous literature (J. M. Li et al., 2023), the parameters for metabolite structure identification were defined as follows: The mass deviation is constrained to a mass tolerance of less than 0.01 Da for first-order spectrum matching, a mass tolerance of less than 0.02 Da for second-order spectrum matching, and a score exceeding 70% for second-order mass spectrometry matching.

2.5. Morris Water Maze (MWM) experiment

The MWM experiment was conducted in accordance with our previous research (Long et al., 2021, 2024). Before commencing the experiment, all rats were continuously trained for 5 days to acquire learning and memory. Following the training period, the navigation test

Table 1
The detailed information about the ingredients of WYD.

Latin name	Chinese name	Botanical part	Provenances	Weight (g)	Batch number
Ginseng Radix Et Rhizoma	Renshen	dried root and rhizome	Jilin	12	2201034
Ziziphi Spinosae Semen	Suanzaoren	dried and ripe seeds	Hebei	12	2112059
Angelicae Sinensis Radix	Danggui	dried root	Gansu	20	2303166
Paeoniae Radix Alba	Baishao	dried root	Anhui	20	2201063
Bambusae Caulis in Taenias	Zhuru	dried intermediate layer of stem	Zhejiang	12	2104044

was conducted, and all rats were given 60 s to reach the platform. For the spatial probe test, all rats had to investigate the area for 60 s after the circular platform was removed. The escape latency was quantified, in conjunction with the total swimming distance, number of platform crossings, and duration spent in the target quadrant, for statistical analysis.

2.6. Hematoxylin-eosin (HE) staining

The hippocampus and cortex were subjected to HE staining to evaluate pathological alterations. Specifically, brain tissue (3 in each group) samples from each experimental group were collected and processed into paraffin-embedded blocks, which were subsequently sectioned. The sections underwent dewaxing in xylene and dehydration through a graded ethanol series (100–75%). After rinsing in double-distilled water, the sections were stained with hematoxylin for 3–5 min, followed by eosin for 5 min. The stained sections were then mounted using neutral gum, photographed, and analyzed with an upright optical microscope (BZ-X800, KEYENCE, Japan).

2.7. Nissl staining

The paraffin-embedded sections were deparaffinized, ethanol dehydrated, and then stained with Nissl stain solution (G1436, Solarbio, China) for 30 min. The stained sections were then scanned and examined using CaseViewer software (version 2.4, 3DHISTECH Ltd., Hungary), with analysis performed using Fiji Image J software (version 1.54, NIH, USA).

2.8. Golgi-Cox staining

Brain tissues (3 in each group) were collected, and Golgi-Cox staining (PK401A, FD NeuroTechnologies, Inc., USA) was performed in accordance with our previous research (Long et al., 2024). Briefly, the mixture of solution A and solution B was prepared. The tissues were soaked in the mixture for 14 days and were then incubated in solution C for 24 h. Next, a freezing microtome (NX70, Thermo Scientific, USA) was utilized to slice the tissues into 100 μm-thick sections. Following a rinse with double-distilled water, the sections were treated with solutions D, E, and F. An Olympus microscope (IXplore SpinSR, Japan) was then used to examine and photograph the stained sections. As described previously (Long et al., 2024), Fiji Image J was used to measure dendritic spine length and density.

2.9. Transmission electron microscope (TEM)

To conduct the TEM examination, hippocampal and cortical tissue (3 in each group) were gathered from each group. Following soaking in 2.5% glut solution (P1126, Solarbio, China) for 24 h, tissues were then treated with 1% osmic acid for 2 h. The tissues were subjected to dehydration and embedding into EMBed 812. A microtome (LN Ultra, RMC Boeckeler, USA) was used to perform ultrathin sections. Afterward, the slices were exposed to a 2.6% lead citrate solution for a duration of 10 min. To examine the synaptic ultrastructure in the hippocampus and cortex, stained sections were viewed under a transmission electron microscope (HT7800, Hitachi, Japan). Consistent with our previous research (Long et al., 2024; Zhao et al., 2024), the dimensions of the postsynaptic density (PSD) were measured with Fiji Image J software.

2.10. Immunofluorescence staining

The dewaxed samples were treated with 5% BSA and incubated for 60 min at ambient temperature. Following PBS washing, the sections were exposed to primary antibodies targeting Aβ (1:400, GB111197, Servicebio, China), GFAP (1:500, GB15100, Servicebio, China), and IBA1(1:500, GB11105, Servicebio, China) for an overnight incubation at 4 °C. The sections were treated with suitable secondary antibodies and left to incubate at room temperature for 50 min. DAPI solution was used to label the nucleus in sections for 10 min, and then coverslipped with an anti-fade mounting medium. Fiji Image J software was utilized to analyze and quantify the fluorescence levels of GFAP and IBA1.

2.11. Immunohistochemistry (ICH) staining

The ICH staining was performed in accordance with previous study (Long et al., 2024). The sections were deparaffinized and dehydrated with de-paraffin liquid or ethanol, respectively. The portions were soaked in antigen retrieval solution that had been boiled to carry out antigen retrieval, then transferred to 5% BSA for a duration of 30 min (SW3015, Solarbio, China). Following incubation, the samples were treated with primary NeuN antibody (1:500, GB11138, Servicebio, China) for one night at 4 °C, then exposed to the secondary antibody (1:200, GB23303, Servicebio, China), and finally stained using the Diaminobenzidine (DAB) substrate kit (G1212, Servicebio, China). Neurons expressing NeuN in the cortex and hippocampus were quantified using Fiji Image J software.

2.12. Enzyme-linked immunosorbent assay (ELISA)

Hippocampal and cortical tissues (5 in each group) were separated and collected. Subsequently, A 9-fold volume of PBS was then added to the tissue for homogenization. Following centrifugation, the supernatant was gathered and utilized to analyze the levels of $A\beta_{1\text{-}40}$ (KE1353, ImmunoWay Biotechnology, USA) and $A\beta_{1\text{-}42}$ (KE1458, ImmunoWay Biotechnology, USA) in the hippocampus and cortex as directed by the manufacturer.

2.13. Western blot

Hippocampal and cortical tissue (3 in each group) were collected in each group, followed by homogenization using RIPA lysis buffer (R0010, Solarbio, China). The homogenized mixture underwent centrifugation at high speed for 10 min (12 000 rpm, 4 °C), resulting in the collection of the supernatant for Western blot analysis. For determining the protein concentrations in the supernatant, Yoche Biotechnology provided a BCA protein assay kit (YSD-500T). Proteins were separated using an 8 % SDS-PAGE gel (G2042, Servicebio, China), and then subsequently moved onto polyvinylidene difluoride membranes (PVDF, WGPVDF45, Servicebio, China). Following washing, the membranes were then blocked with a 5% skim milk solution in PBST for 2 h, and subsequently exposed to primary antibodies diluted in PBST overnight at 4 °C. Table 2 displays comprehensive details regarding the antibodies utilized in this research. Following the PBST wash, the membranes were then exposed to secondary antibodies for 1 h, followed by ECL reagent (G2014, Servicebio, China) to capture the blots. The membranes were scanned with a Chemiluminescence imager (SCG-W2000, Servicebio, China) and band intensities were analyzed and quantified with Fiji Image J software.

2.14. Statistical analysis

GraphPad Prism software (version 9.0, GraphPad Software Inc, USA) was used to analyze the experimental data, and experimental data were presented as mean ± standard error of mean (SEM). Normality and Lognormality Tests were performed on all data. One-way ANOVA with LSD or Tamhane T2 test was used for normally distributed data, while Kruskal-Wallis H test was used for non-normally distributed data. Statistical significance was defined as $P < 0.05$.

Table 2
The antibodies used in Western blot analysis were thoroughly described.

Antibodies	Catalog number	Host	Dilution	Provider
ADAM10	GB11318	Rabbit	1:1000	Servicebio
BACE1	A11533	Rabbit	1:1000	ABclonal Biotechnology
PS1	GB11779	Rabbit	1:1000	Servicebio
IDE	GB111387	Rabbit	1:1000	Servicebio
PSD95	A0131	Rabbit	1:1000	ABclonal Biotechnology
SYN1	A17362	Rabbit	1:1000	ABclonal Biotechnology
TNF-α	GB11188	Rabbit	1:500	Servicebio
IL-1β	GB11113	Rabbit	1:1000	Servicebio
IL-6	GB11117	Rabbit	1:1000	Servicebio
SIRT1	A11267	Rabbit	1:1000	ABclonal Biotechnology
Nrf2	GB113808	Rabbit	1:1000	Servicebio
IκBα	GB13212	Rabbit	1:1000	Servicebio
p-IκBα-Ser32	AP0707	Rabbit	1:1000	ABclonal Biotechnology
NF-κB p65	GB11997	Rabbit	1:1000	Servicebio
p-NF-κB p65-Ser536	GB113882	Rabbit	1:500	Servicebio
β-actin	AC026	Rabbit	1:100 000	ABclonal Biotechnology

3. Results

3.1. The identified compounds in WYD extract

UHPLC-MS/MS analysis identified a total of 99 active ingredients in the WYD extract. Detailed information regarding these active ingredients is provided in Fig. 2 and Table 3. According to Table 3, the active ingredients predominantly originate from Ginseng Radix Et Rhizoma, Ziziphi Spinosae Semen, Angelicae Sinensis Radix and Paeoniae Radix Alba. Specifically, the active ingredients identified in Ginseng Radix Et Rhizoma

Include various ginsenoside compounds, such as Ginsenoside Rg1, Ginsenoside Rb1, Ginsenoside Rb2, Ginsenoside Rg5, and Ginsenoside Re. The primary constituents identified in Ziziphi Spinosae Semen are saponins and flavonoids, specifically Jujuboside A, Jujuboside B, and Spinosin. The active ingredients in Angelicae Sinensis Radix are mainly organic acids, such as Chlorogenic acid, Homovanillic acid, and Linoleic acid. Additionally, the active compounds in Paeoniae Radix Alba predominantly consist of terpenoids, and organic acids, including Albiflorin, Gallic acid, and Oleanolic acid.

3.2. WYD ameliorates learning and memory impairment of CSD rats

MWM experiment has been generally acknowledged as an effective method to evaluate the cognitive function in rodents. Therefore, we adopt this test to investigate whether WYD could alleviate the cognitive decline induced by CSD. During the 5 days training period, all rats participated in learning and memory tasks. Analysis of the data in Fig. 3A revealed that there was no significant difference in latency for rats from the first to fourth day in all groups ($P > 0.05$). However, a noticeable increase in latency was observed in the Model group by fifth day as compared to the Control group, while the M-WYD group experienced a significant reduction ($P < 0.01$ or 0.05, Fig. 3A). Upon completion of the acquired training, we re-evaluated the escape latency of rats. The Model group had higher latency compared to the Control group, while the M-WYD group had lower latency ($P < 0.01$, Fig. 3B). The L-WYD and H-WYD groups, however, were not significantly different from the Model group about escape latency ($P > 0.05$, Fig. 3B). Fig. 3C illustrated a notable disparity in total swimming distance between the Model group and the Control group ($P < 0.01$), and the M-WYD group reduced the total swimming distance over the Model group ($P < 0.05$). Unfortunately, L-WYD and H-WYD groups did not significantly reverse the above-mentioned experimental results ($P > 0.05$, Fig. 3BandC). In the spatial probe test, rats' spatial memory was assessed by comparing the number of platform crossings, and time within the target quadrant. Fig. 3D shows that the Model group crossed the platform less than the Control group, but the M-WYD group reversed this

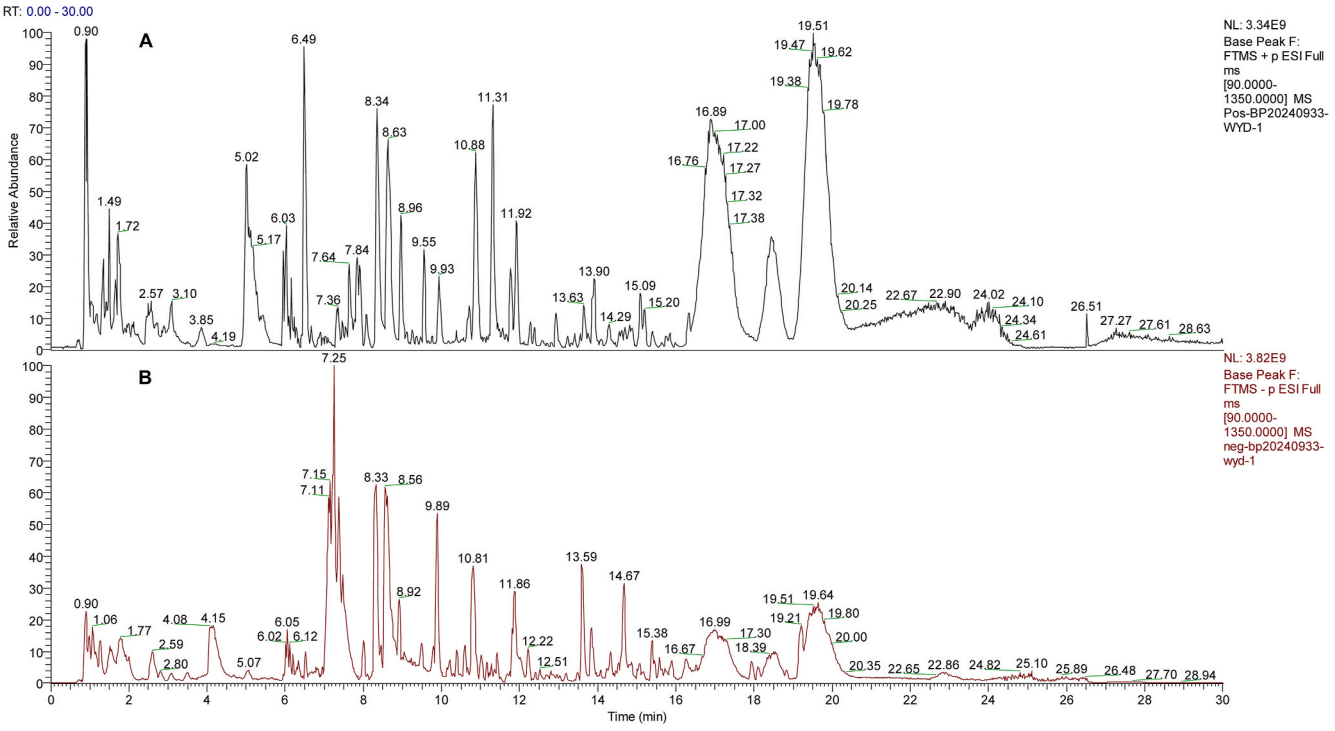

Fig. 2. In HPLC-MS/MS analysis, the fingerprint of WYD extract has been determined in two ways. (A) The positive ion modes of WYD extract have been detected. (B) The negative ion modes of WYD extract have been detected.

Table 3
The detailed information on active ingredients in WYD extract by UHPLC-MS/MS analysis.

No.	t_R (min)	Formula	Measured (m/z)	Compound	Source
1	10.876	$C_{23}H_{28}O_{11}$	481.12 $[M+H]^+$	Albiflorin	Paeoniae Radix Alba
2	4.061	$C_7H_6O_5$	169.01 $[M-H]^-$	Gallic Acid	Paeoniae Radix Alba
3	10.326	$C_{41}H_{32}O_{26}$	939.11 $[M-H]^-$	Pentagalloylglucose	Paeoniae Radix Alba
4	7.233	$C_{15}H_{26}O$	245.18 $[M+Na]^+$	Nerolidol	Paeoniae Radix Alba
5	17.609	$C_{10}H_{16}O$	175.11 $[M+Na]^+$	Perillyl alcohol	Paeoniae Radix Alba
6	0.777	$C_8H_8O_5$	185.04 $[M+H]^+$	Gallic acid methyl ester	Paeoniae Radix Alba
7	10.866	$C_{21}H_{20}O_{11}$	447.09 $[M-H]^-$	Kaempferol 7-O-glucoside	Paeoniae Radix Alba
8	8.290	$C_7H_6O_2$	121.03 $[M-H]^-$	Benzoic acid	Paeoniae Radix Alba
9	10.424	$C_{30}H_{32}O_{15}$	631.16 $[M-H]^-$	Galloylpaeoniflorin	Paeoniae Radix Alba
10	22.844	$C_{16}H_{32}O_3$	271.23 $[M-H]^-$	16-Hydroxypalmitic acid	Paeoniae Radix Alba
11	10.370	$C_{21}H_{20}O_{11}$	449.11 $[M+H]^+$	Astragalin	Paeoniae Radix Alba
12	6.944	$C_{15}H_{14}O_7$	305.06 $[M-H]^-$	Epigallocatechin	Paeoniae Radix Alba
13	7.620	$C_{27}H_{24}O_{18}$	635.08 $[M-H]^-$	Gallotannin	Paeoniae Radix Alba
14	7.339	$C_{10}H_{14}O$	151.11 $[M+H]^+$	Myrtenal	Paeoniae Radix Alba
15	18.795	$C_{14}H_{22}O$	205.16 $[M-H]^-$	2,4-di-tert-butylphenol	Paeoniae Radix Alba
16	10.321	$C_{27}H_{30}O_{15}$	593.15 $[M-H]^-$	Kaempferol 3-O-rutinoside	Paeoniae Radix Alba
17	10.838	$C_9H_{16}O_4$	187.10 $[M-H]^-$	Azelaic acid	Angelicae Sinensis Radix
18	6.688	$C_8H_8O_2$	135.04 $[M-H]^-$	Phenylacetic acid	Angelicae Sinensis Radix
19	6.838	$C_8H_8O_3$	151.04 $[M-H]^-$	Anisic acid	Angelicae Sinensis Radix
20	2.627	$C_4H_4N_2O_2$	113.03 $[M+H]^+$	Uracil	Angelicae Sinensis Radix
21	9.167	$C_8H_8O_3$	153.05 $[M+H]^+$	Vanillin	Angelicae Sinensis Radix
22	0.935	$C_4H_6N_4O_3$	181.03 $[M+Na]^+$	Allantoin	Angelicae Sinensis Radix
23	23.829	$C_{20}H_{30}O$	269.23 $[M + H\text{-}H_2O]^+$	Retinol	Angelicae Sinensis Radix
24	4.703	$C_{12}H_{20}O_2$	219.13 $[M+Na]^+$	Linalyl acetate	Angelicae Sinensis Radix
25	8.070	$C_9H_8O_4$	163.04 $[M + H\text{-}H_2O]^+$	Caffeic acid	Angelicae Sinensis Radix
26	10.328	$C_{21}H_{18}O_{11}$	447.09 $[M+H]^+$	baicalin	Angelicae Sinensis Radix
27	7.787	$C_8H_8O_4$	167.03 $[M-H]^-$	Vanillic acid	Angelicae Sinensis Radix
28	13.585	$C_{10}H_{10}O_4$	177.05 $[M + H\text{-}H_2O]^+$	Isoferulic acid	Angelicae Sinensis Radix
29	7.838	$C_{11}H_{12}O_4$	191.07 $[M + H\text{-}H_2O]^+$	Dimethylcaffeic Acid	Angelicae Sinensis Radix
30	11.006	$C_{16}H_{18}O_9$	353.09 $[M-H]^-$	Cryptochlorogenic acid	Angelicae Sinensis Radix
31	10.638	$C_{16}H_{18}O_9$	353.09 $[M-H]^-$	Chlorogenic acid	Angelicae Sinensis Radix
32	7.587	$C_8H_6O_4$	165.02 $[M-H]^-$	Phthalic acid	Angelicae Sinensis Radix
33	9.376	$C_{10}H_{10}O_3$	161.06 $[M + H\text{-}H_2O]^+$	4-Methoxycinnamic acid	Angelicae Sinensis Radix
34	0.624	$C_9H_{10}O_4$	183.06 $[M+H]^+$	Homovanillic acid	Angelicae Sinensis Radix
35	19.195	$C_{12}H_{14}O_2$	191.11 $[M+H]^+$	Ligustilide	Angelicae Sinensis Radix
36	11.894	$C_{42}H_{72}O_{14}$	845.49 $[M + FA\text{-}H]^-$	Ginsenoside Rg1	Ginseng Radix Et Rhizoma
37	14.770	$C_{53}H_{90}O_{22}$	1123.58 $[M + FA\text{-}H]^-$	Ginsenoside Rb2	Ginseng Radix Et Rhizoma
38	11.827	$C_{48}H_{82}O_{18}$	991.54 $[M + FA\text{-}H]^-$	Ginsenoside Re	Ginseng Radix Et Rhizoma
39	14.265	$C_{54}H_{92}O_{23}$	1153.59 $[M + FA\text{-}H]^-$	Ginsenoside Rb1	Ginseng Radix Et Rhizoma
40	14.838	$C_{48}H_{76}O_{19}$	955.48 $[M-H]^-$	Ginsenoside Ro	Ginseng Radix Et Rhizoma
41	15.303	$C_{36}H_{62}O_9$	683.43 $[M + HCOO]^-$	Ginsenoside F1	Ginseng Radix Et Rhizoma
42	14.590	$C_{42}H_{72}O_{13}$	829.5 $[M + FA\text{-}H]^-$	Ginsenoside Rg2	Ginseng Radix Et Rhizoma
43	16.059	$C_{48}H_{82}O_{18}$	991.54 $[M + HCOO]^-$	Ginsenoside B2	Ginseng Radix Et Rhizoma
44	13.83	$C_{42}H_{72}O_{14}$	799.48 $[M-H]^-$	Ginsenoside Rf	Ginseng Radix Et Rhizoma
45	17.932	$C_{42}H_{72}O_{13}$	783.48 $[M-H]^-$	Ginsenoside Rg3	Ginseng Radix Et Rhizoma
46	19.848	$C_{42}H_{70}O_{12}$	765.47 $[M-H]^-$	Ginsenoside Rg5	Ginseng Radix Et Rhizoma
47	1.308	$C_{18}H_{32}O_{16}$	503.16 $[M-H]^-$	Raffinose	Ginseng Radix Et Rhizoma
48	11.868	$C_{30}H_{52}O_4$	459.38 $[M + H\text{-}H_2O]^+$	Panaxatriol	Ginseng Radix Et Rhizoma
49	15.364	$C_{47}H_{74}O_{18}$	925.47 $[M-H]^-$	Chikusetsusaponin iv	Ginseng Radix Et Rhizoma
50	14.884	$C_{15}H_{20}O_4$	265.14 $[M+H]^+$	Vulgarin	Ginseng Radix Et Rhizoma
51	4.871	$C_{10}H_{13}N_5O_4$	266.09 $[M-H]^-$	Adenosine	Ginseng Radix Et Rhizoma
52	8.200	$C_{10}H_{16}N_2O_3S$	243.09 $[M-H]^-$	Biotin	Ginseng Radix Et Rhizoma
53	0.969	$C_4H_6O_5$	133.01 $[M-H]^-$	Malic acid	Ginseng Radix Et Rhizoma
54	6.268	$C_{20}H_{19}NO_5$	376.12 $[M+Na]^+$	Protopine	Ginseng Radix Et Rhizoma
55	15.271	$C_6H_{12}O_5$	187.06 $[M+Na]^+$	Rhamnose	Ginseng Radix Et Rhizoma
56	8.070	$C_9H_{10}O_5$	181.05 $[M + H\text{-}H_2O]^+$	Syringic acid	Ginseng Radix Et Rhizoma
57	9.153	$C_9H_8O_2$	131.05 $[M\text{-}H_2O + H]^+$	Cinnamic acid	Ginseng Radix Et Rhizoma
58	6.235	$C_7H_6O_3$	137.02 $[M-H]^-$	4-Hydroxybenzoic acid	Ginseng Radix Et Rhizoma
59	9.566	$C_{28}H_{32}O_{15}$	609.18 $[M+H]^+$	Spinosin	Ziziphi Spinosae Semen
60	17.430	$C_{38}H_{40}O_{18}$	783.23 $[M-H]^-$	6‴-Feruloylspinosin	Ziziphi Spinosae Semen
61	10.121	$C_{22}H_{22}O_{10}$	447.13 $[M+H]^+$	Calycosin 7-O-glucoside	Ziziphi Spinosae Semen
62	14.287	$C_{30}H_{50}O_2$	425.38 $[M + H\text{-}H_2O]^+$	betulin	Ziziphi Spinosae Semen
63	7.899	$C_{17}H_{19}NO_3$	286.14 $[M+H]^+$	Coclaurine	Ziziphi Spinosae Semen
64	9.508	$C_{27}H_{30}O_{16}$	609.14 $[M-H]^-$	Rutin	Ziziphi Spinosae Semen
65	19.038	$C_{20}H_{40}O_2$	357.28 $[M-H+2Na]^+$	Arachidic acid	Ziziphi Spinosae Semen
66	8.700	$C_{20}H_{24}NO_4$	342.17 $[M+H]^+$	Magnoflorine	Ziziphi Spinosae Semen
67	9.905	$C_{21}H_{20}O_{10}$	431.10 $[M-H]^-$	Isovitexin	Ziziphi Spinosae Semen
68	6.049	$C_{20}H_{20}O_5$	363.12 $[M+Na]^+$	Licoflavanone	Ziziphi Spinosae Semen
69	12.979	$C_{16}H_{12}O_5$	285.07 $[M+H]^+$	Calycosin	Ziziphi Spinosae Semen
70	23.456	$C_{20}H_{32}O_2$	305.25 $[M+H]^+$	Arachidonic acid	Ziziphi Spinosae Semen
71	26.34	$C_{58}H_{94}O_{26}$	1205.61 $[M-H]^-$	Jujuboside A	Ziziphi Spinosae Semen
72	28.96	$C_{52}H_{84}O_{21}$	1089.55 $[M + HCOO]^-$	Jujuboside B	Ziziphi Spinosae Semen
73	14.607	$C_{17}H_{14}O_7$	331.08 $[M+H]^+$	Tricin	Bambusae Caulis in Taenias
74	9.535	$C_9H_{10}O_4$	181.05 $[M-H]^-$	Syringaldehyde	Bambusae Caulis in Taenias

(*continued on next page*)

Table 3 (*continued*)

No.	t_R (min)	Formula	Measured (m/z)	Compound	Source
75	11.055	$C_{10}H_{10}O_3$	179.07 $[M+H]^+$	Coniferaldehyde	Bambusae Caulis in Taenias
76	9.406	$C_9H_8O_3$	147.04 $[M + H\text{-}H_2O]^+$	p-Coumaric acid	Bambusae Caulis in Taenias
77	9.972	$C_{10}H_{10}O_4$	177.06 $[M + H\text{-}H_2O]^+$	Ferulic acid	Angelicae Sinensis Radix/Ziziphi Spinosae Semen
78	1.619	$C_5H_5N_5$	134.05 $[M\text{-}H]^-$	Adenine	Angelicae Sinensis Radix/Ginseng Radix Et Rhizoma
79	0.937	$C_5H_{14}NO$	104.11 $[M]^+$	Choline	Angelicae Sinensis Radix/Ginseng Radix Et Rhizoma
80	5.908	$C_{10}H_{13}N_5O_5$	282.08 $[M\text{-}H]^-$	Guanosine	Angelicae Sinensis Radix/Ginseng Radix Et Rhizoma
81	1.832	$C_6H_5NO_2$	124.04 $[M+H]^+$	Nicotinic acid	Angelicae Sinensis Radix/Ginseng Radix Et Rhizoma
82	10.463	$C_9H_{12}N_2O_6$	245.077 $[M+H]^+$	Uridine	Angelicae Sinensis Radix/Ginseng Radix Et Rhizoma
83	8.136	$C_{15}H_{14}O_6$	291.09 $[M+H]^+$	Epicatechin	Ziziphi Spinosae Semen/Ginseng Radix Et Rhizoma
84	1.784	$C_6H_8O_7$	191.02 $[M\text{-}H]^-$	Citric acid	Bambusae Caulis in Taenias/Ginseng Radix Et Rhizoma
85	2.531	C_6H_6O	95.05 $[M+H]^+$	Phenol	Angelicae Sinensis Radix/Paeoniae Radix Alba
86	10.110	$C_{10}H_{16}$	137.13 $[M+H]^+$	Myrcene	Angelicae Sinensis Radix/Paeoniae Radix Alba
87	11.726	$C_{30}H_{48}O_3$	439.36 $[M + H\text{-}H_2O]^+$	Betulinic acid	Paeoniae Radix Alba/Ziziphi Spinosae Semen
88	14.818	$C_{30}H_{48}O_3$	439.36 $[M + H\text{-}H_2O]^+$	Oleanolic acid	Ziziphi Spinosae Semen/Paeoniae Radix Alba
89	7.356	$C_{15}H_{14}O_6$	289.07 $[M\text{-}H]^-$	Catechin	Paeoniae Radix Alba/Ziziphi Spinosae Semen
90	19.691	$C_{16}H_{22}O_4$	277.14 $[M\text{-}H]^-$	Dibutyl phthalate	Paeoniae Radix Alba/Ginseng Radix Et Rhizoma
91	6.880	$C_9H_{10}O_3$	167.07 $[M+H]^+$	Paeonol	Paeoniae Radix Alba/Ginseng Radix Et Rhizoma
92	10.907	$C_7H_6O_3$	137.02 $[M\text{-}H]^-$	Salicylic acid	Paeoniae Radix Alba/Ginseng Radix Et Rhizoma
93	24.627	$C_{18}H_{34}O_2$	281.25 $[M\text{-}H]^-$	Oleic acid	Angelicae Sinensis Radix/Ziziphi Spinosae Semen/Ginseng Radix Et Rhizoma
94	17.963	$C_{16}H_{32}O_2$	255.23 $[M\text{-}H]^-$	Palmitic acid	Paeoniae Radix Alba/Angelicae Sinensis Radix/Ginseng Radix Et Rhizoma
95	10.005	$C_{10}H_8O_4$	193.05 $[M+H]^+$	Scopoletin	Paeoniae Radix Alba/Angelicae Sinensis Radix/Bambusae Caulis in Taenias
96	10.370	$C_{15}H_{10}O_6$	287.05 $[M+H]^+$	Kaempferol	Paeoniae Radix Alba/Ziziphi Spinosae Semen/Ginseng Radix Et Rhizoma
97	1.387	$C_{12}H_{22}O_{11}$	341.11 $[M\text{-}H]^-$	Sucrose	Paeoniae Radix Alba/Bambusae Caulis in Taenias/Ginseng Radix Et Rhizoma
98	13.681	$C_9H_6O_3$	163.04 $[M+H]^+$	Umbelliferone	Angelicae Sinensis Radix/Paeoniae Radix Alba
99	23.717	$C_{18}H_{32}O_2$	279.23 $[M\text{-}H]^-$	Linoleic acid	Angelicae Sinensis Radix/Ziziphi Spinosae Semen/Paeoniae Radix Alba

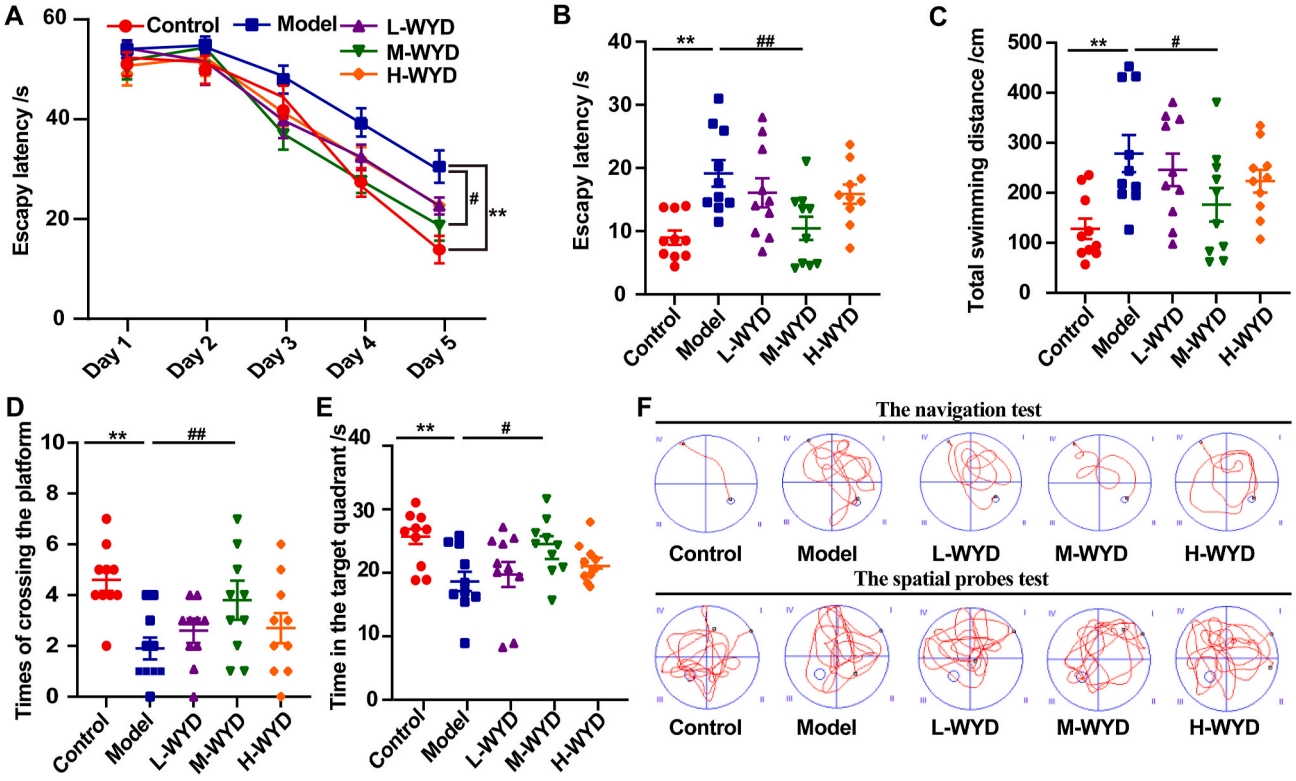

Fig. 3. Effect of WYD on CSD-induced cognitive decline. (A) A 5-day training period was used to calculate escape latency for different groups. (B) Results from the navigation test indicate variations in escape latency among different groups. (C) The graph shows the total swimming distance in the navigation test for different groups. (D) The graph depicts the frequency of platform crossings by rats during the spatial probe test. (E) The graph shows the amount of time spent in quadrant by rats during the spatial probe test. (F) Representative trajectory images of different groups in the navigation and spatial probe tests, respectively.Data are shown as mean ± SEM (n = 10/group).

Data are shown as mean ± SEM. **P < 0.01 compared toData are shown as mean ± SEM (n = 10/group). Control group; #P < 0.05 or ##P < 0.01 compared to Model group.

trend ($P < 0.01$). The Model group exhibited significantly less time in the target quadrant compared to the Control group, whereas the M-WYD group demonstrated a notable increase in time spent in the target quadrant relative to the Model group ($P < 0.01$ or 0.05, Fig. 3E). Conversely, the L-WYD and H-WYD groups did not show a comparable level of effectiveness as the M-WYD group in these specific measures ($P > 0.05$, Fig. 3DandE). These findings indicated that the WYD, particularly the M-WYD, could improve cognitive function and memory deficits

caused by CSD.

3.3. WYD reduces neuronal damage in the hippocampus and cortex of CSD rats

Neurons play a crucial role in cognitive function, and emerging evidence indicate that CSD can damage and lose neurons, ultimately lead to cognitive decline (Cao et al., 2019; Lyons et al., 2023; X. Wang et al., 2023). To investigate the potential protective effects of WYD, HE and Nissl staining was used to assess neuronal damage in the hippocampus and cortex. HE staining demonstrated that neurons in the hippocampal CA3 region and cortex of the Model group exhibited signs of degeneration relative to the Control group, including darker, distorted, and degenerated nuclei (Fig. 4A). Conversely, the M-WYD group displayed

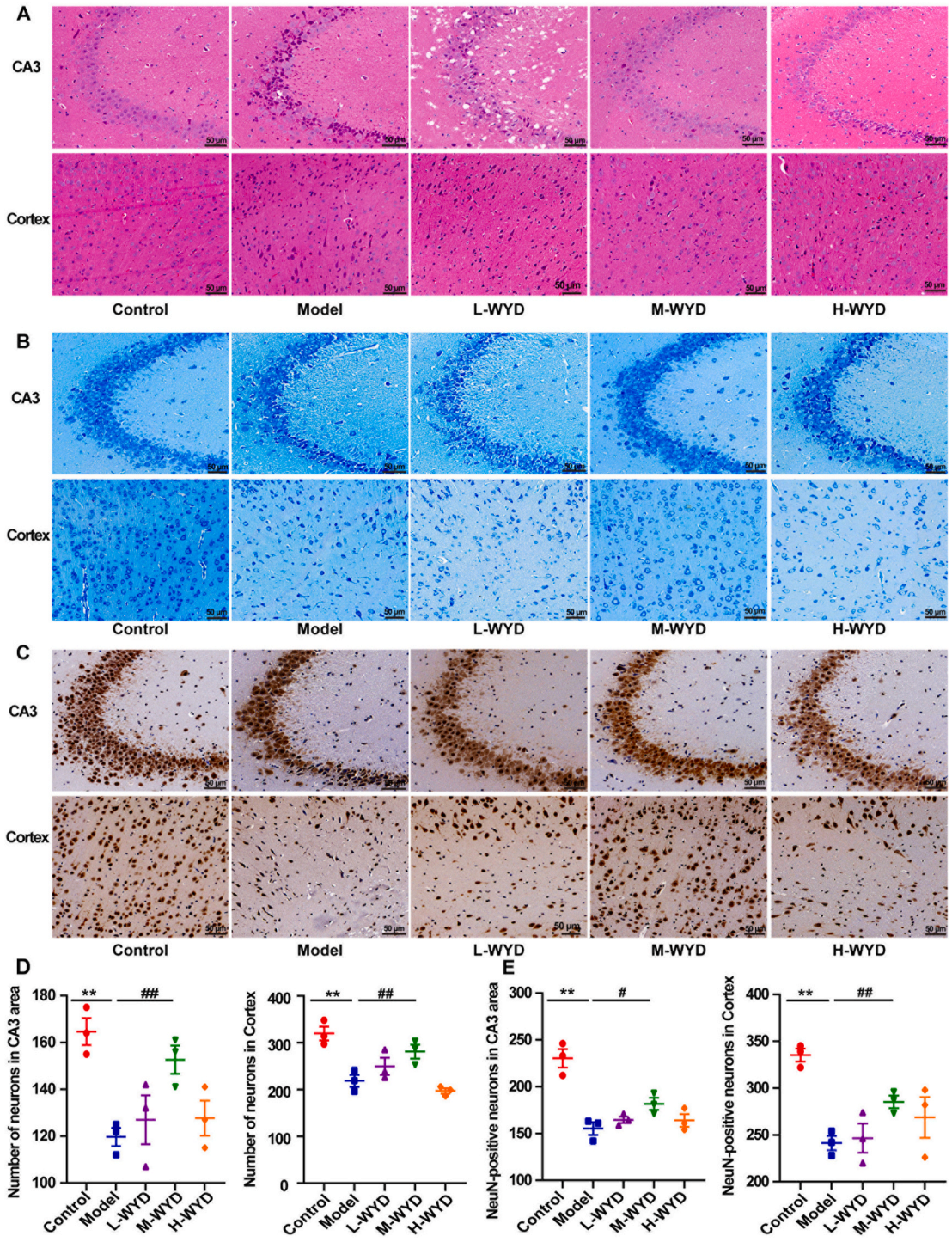

Fig. 4. Effect of WYD on CSD-induced neuronal damage. (A) HE staining was performed on the hippocampal CA3 region and the cortex, with a scale bar of 50 μm. (B) Nissl staining was conducted in the hippocampal CA3 region and cortex, with a scale bar of 50 μm. (C) Immunohistochemical staining for the neuronal marker NeuN was performed in the hippocampal CA3 region and cortex, with a scale bar of 50 μm. (D) An assessment of the neuronal count in the CA3 area of the hippocampus and cortex (n = 3). (E) The CA3 area of the hippocampus and cortex was quantified for NeuN-expressing cells (n = 3).
Data are shown as mean ± SEM. **P < 0.01 compared to Control group; #P < 0.05 or ##P < 0.01 compared to Model group.

reduced neuronal damage in these regions, with an improved appearance of both the stained neurons and their nuclei. Nissl staining revealed that neurons in the hippocampal CA3 region and cortex of the Model group exhibited distinct staining patterns, characterized by deformed and altered cell bodies, as illustrated in Fig. 4B. In contrast, the groups treated with WYD, especially the M-WYD group, demonstrated a reduction in these morphological alterations. Meanwhile, number of neurons were quantified to execute statistical analysis. As compared to the Control group, CSD led to a decrease in neurons in the CA3 region of the hippocampus and cortex ($P < 0.01$, Fig. 4B and D). However,

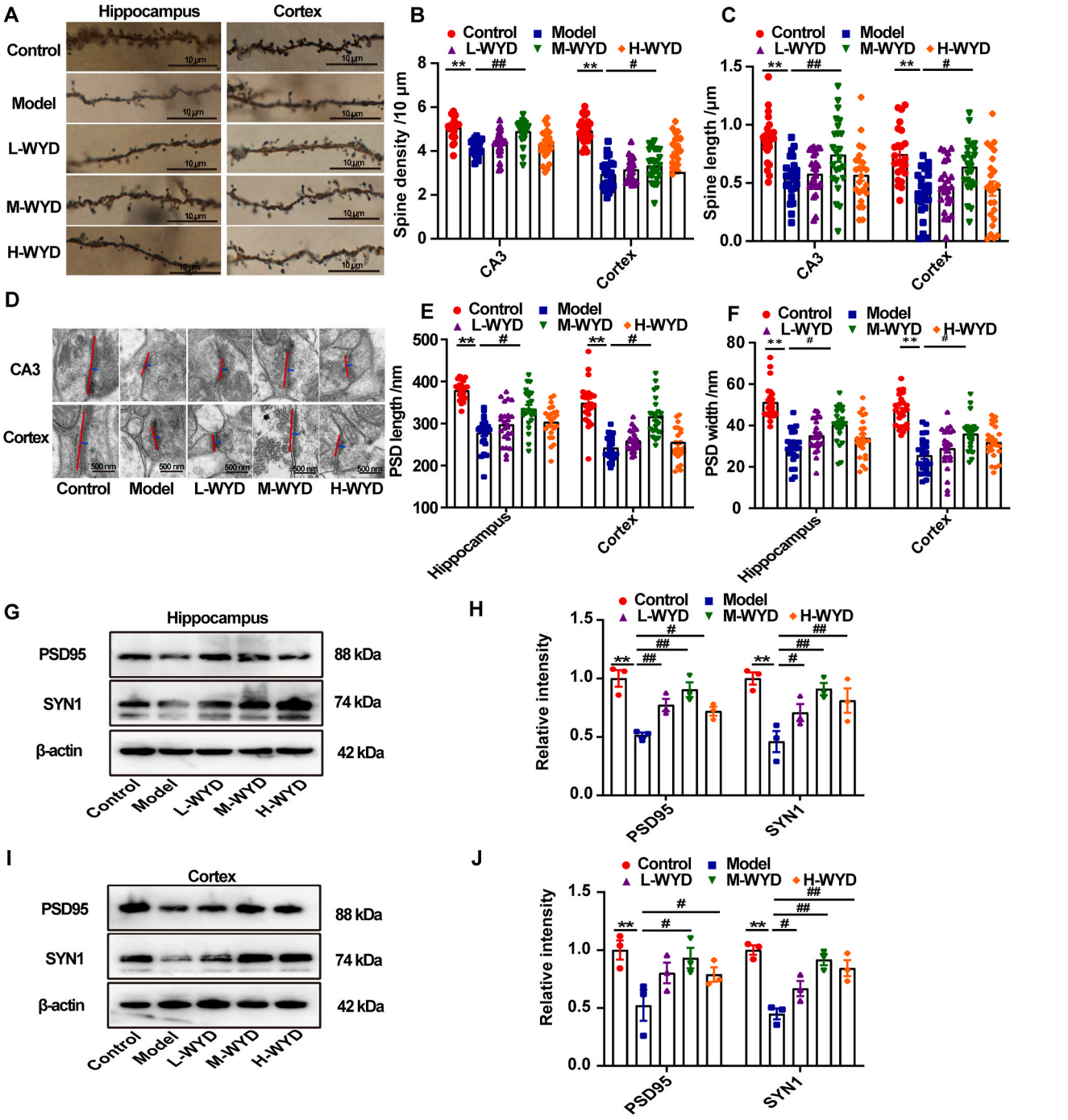

Fig. 5. Impact of WYD on CSD-induced synaptic dysfunction. (A) Illustrative images of Golgi-Cox staining in the CA3 region of the hippocampus and cortex are presented, with a scale bar indicating a measurement of 10 μm. (B) The quantitative analysis of spine density was conducted in the CA3 region of the hippocampus and cortex (n = 3, each sample should include a random selection of 8–10 dendrites for subsequent analysis.). (C) The quantitative analysis of spine length was conducted in the CA3 region of the hippocampus and cortex (n = 3, each sample should include a random selection of 8–10 dendrites for subsequent analysis). (D) Representative TEM images of the hippocampal CA3 region and cortex are shown, with a scale bar indicating a length of 500 nm (Red and blue lines indicate the PSD's length and width, respectively). (E) The length of PSD in hippocampal CA3 region and cortex (n = 3, a total of 8–10 synapses should be randomly selected from each sample for analysis). (F) The width of PSD in hippocampal CA3 region and cortex (n = 3, a total of 8–10 synapses should be randomly selected from each sample for analysis). (G) Electrophoretic patterns of PSD95 and SYN1 in the hippocampus. (H) Quantitative assessment of PSD95 and SYN1 in the hippocampus (n = 3). (I) Electrophoretic patterns of PSD95 and SYN1 in the cortex. (J) Quantitative assessment of PSD95 and SYN1 in the cortex (n = 3).
Data are shown as mean ± SEM. **P < 0.01 compared to Control group; #P < 0.05 or ##P < 0.01 compared to Model group.

M-WYD was able to restore the reduced neuron count in these areas when compared to the Model group ($P < 0.01$, Fig. 4B and D). A discrepancy in neuron count was not apparent when compared to the Model group between L-WYD and H-WYD ($P > 0.05$, Fig. 4B and D). Subsequently, immunohistochemistry for NeuN was employed to label the neurons. A noticeable decrease in NeuN-positive neurons was observed in the hippocampal CA3 region and cortex with CSD, but this was reversed by the administration of M-WYD ($P < 0.01$ or 0.05, Fig. 4C and E). Immunohistochemistry revealed no significant increase in the number of neurons in the hippocampal CA3 region or cortex of the L-WYD and H-WYD groups compared to the Model group ($P > 0.05$, Fig. 4C and E), consistent with Nissl staining results. These findings

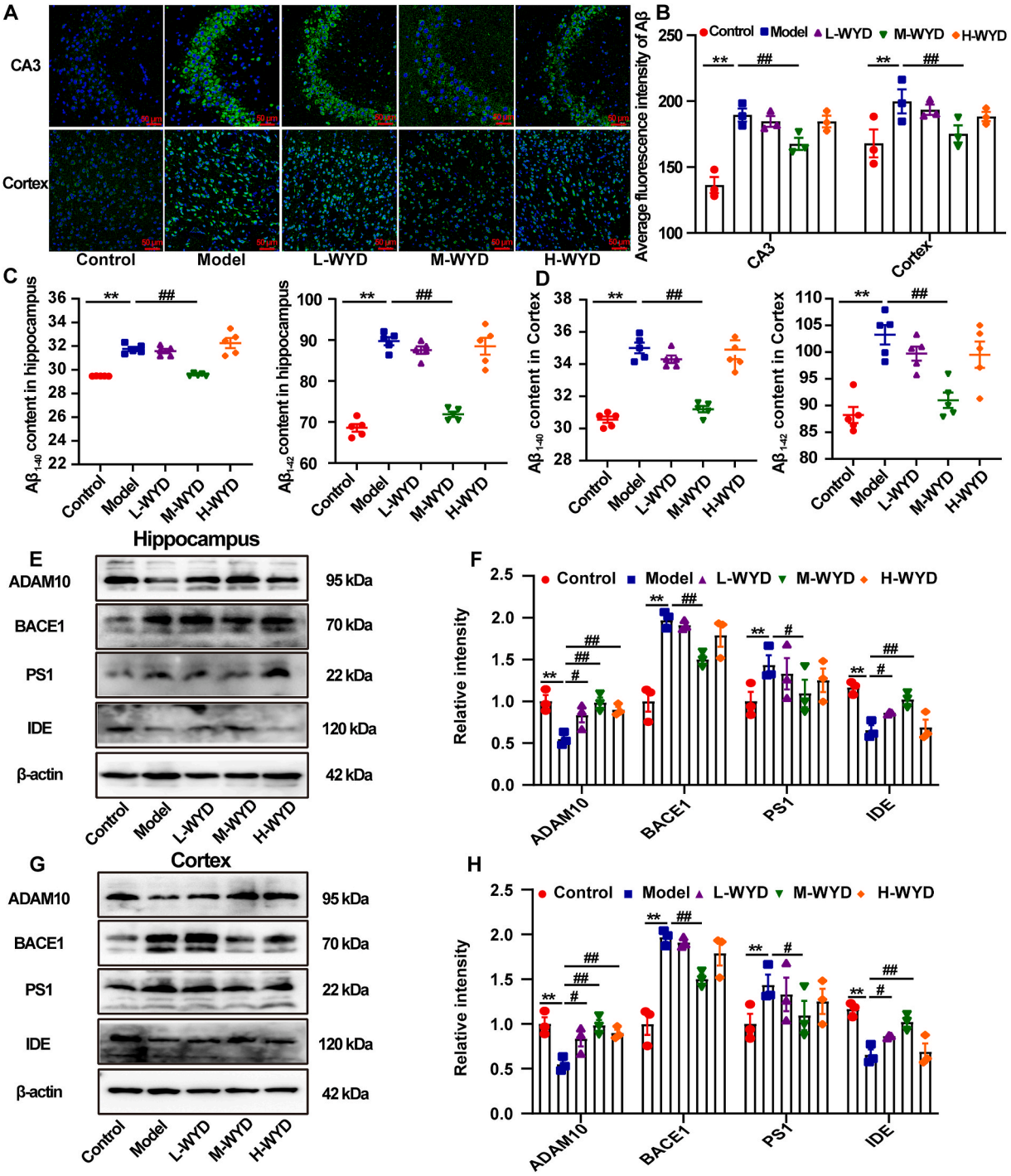

Fig. 6. CSD-induced Aβ production was inhibited by WYD via regulating Aβ-related enzymes. (A) Immunofluorescence staining was conducted to detect the presence of Aβ in the hippocampal CA3 region and cortex, with a scale bar of 50 μm. (B) Fluorescence intensity of Aβ in hippocampal CA3 region and cortex (n = 3). (C) The levels of hippocampal $Aβ_{1-40}$ and $Aβ_{1-42}$ expression were measured (n = 5). (D) Cortical $Aβ_{1-40}$ and $Aβ_{1-42}$ expression level were quantified (n = 5). (E) The hippocampus demonstrated electrophoretic bands for ADAM10, BACE1, PS1 and IDE. (F) Hippocampus-specific quantitative analyses for ADAM10, BACE1, PS1 and IDE (n = 3). (G) The cortex demonstrated electrophoretic bands for ADAM10, BACE1, PS1 and IDE. (H) Quantitative analysis for ADAM10, BACE1, PS1 and IDE in the cortex (n = 3).
Data are shown as mean ± SEM. **P < 0.01 compared to Control group; #P < 0.05 or ##P < 0.01 compared to Model group.

suggest that WYD effectively reduces neuronal damage and loss in CSD rats.

3.4. WYD reduces the synaptic dysfunction in the hippocampus and cortex of CSD rats

The synapse, a fundamental structural and functional component of neurons, supports cognitive formation. Dendritic spines are essential for maintaining synaptic junctions and transmitting signals between synapses. Previous studies have confirmed that CSD can cause structural and functional damage of dendritic spines (H. Gao et al., 2023; Z. R. Li et al., 2022; Zhang et al., 2023). Therefore, we employed Golgi-Cox staining to mark and observe the dendritic spines in the hippocampus and cortex, dendritic spine density and length was then quantified. Fig. 5A–C showed a significant reduction in both the density and length of dendritic spines in the hippocampal CA3 region and cortex following CSD compared to the Control group ($P < 0.01$). Conversely, administration of M-WYD resulted in a notable increase in these parameters ($P < 0.01$ or 0.05, Fig. 5A–C). However, L-WYD and H-WYD did not have similar neuroprotective effects as M-WYD, a finding consistent with results from Nissl staining and immunohistochemistry ($P > 0.05$, Fig. 5A–C). We used TEM to analyze the synaptic structure in the hippocampal CA3 area and cortex, measuring the dimensions of the PSD with Image J software. A significant reduction in PSD dimensions was observed in the CSD group relative to the Control group, and these reductions were restored by M-WYD ($P < 0.01$ or 0.05, Fig. 5D–F). No statistically significant differences were found between the L-WYD and H-WYD groups in comparison to the Model group, as the PSD length and width did not show significant increases ($P > 0.05$, Fig. 5D–F). The protective effect of WYD on synapses was additionally verified through the detection and quantification of synaptic function-related proteins, including PSD95 and SYN1. CSD rats treated with WYD showed increased PSD95 and SYN1 protein levels in the hippocampus and cortex, with the M-WYD group showing higher levels than the L-WYD and H-WYD groups ($P < 0.01$ or 0.05, Fig. 5G–J). The findings presented above indicate that WYD may contribute to the mitigation of synaptic dysfunction in CSD rats.

3.5. WYD reduces the Aβ production in the hippocampus and cortex of CSD rats through regulating Aβ-related enzymes

Recent studies have indicated that CSD enhances production of Aβ in brains, while sleep disturbances accelerate and worsen Aβ deposition in AD models (Beiyu et al., 2024; Liu et al., 2022; C. Wang et al., 2021). Moreover, relevant clinical studies have shown that patients with sleep disorders have a significantly higher Aβ expression level than normal (Ye et al., 2023). Aβ is widely known to trigger neurotoxicity, so we employed immunofluorescence for Aβ to investigate the mechanism that WYD ameliorated neuronal and synaptic damage in CSD rats. Immunofluorescence staining indicated an elevated expression of Aβ in the hippocampus and cortex of the Model group compared to the Control group ($P < 0.01$, Fig. 6AandB). However, administration of M-WYD significantly reduced these elevated Aβ levels ($P < 0.01$, Fig. 6AandB). Given that Aβ predominantly exists in the isoforms $Aβ_{1-40}$ and $Aβ_{1-42}$, we quantified the levels of these proteins in the hippocampus and cortex using ELISA kits. Fig. 6C andD illustrate a significant elevation in the levels of $Aβ_{1-40}$ and $Aβ_{1-42}$ in the hippocampus and cortex subsequent to CSD, as compared to the Control group ($P < 0.01$). The administration of M-WYD effectively mitigated this increase ($P < 0.01$, Fig. 6C andD). However, no statistically significant differences in above-mentioned aspects were observed between the L-WYD and H-WYD groups in comparison to the Model group ($P > 0.05$, Fig. 6A–D). Previous research (Chen et al., 2017; Hao et al., 2023; Y. Y. Li et al., 2023) have established that Aβ production is predominantly regulated by Aβ-related enzymes, specifically α-, β- and γ-related secretase (ADAM10, BACE1, PS1, respectively), as well as the insulin degrading enzyme (IDE). In our investigation, we employed Western blot to quantify these protein levels in the hippocampus and cortex. The CSD exhibited significantly decreased expression levels of ADAM10 and IDE in the hippocampus and cortex relative to the Control group, and this trend was reversed by M-WYD ($P < 0.01$ or 0.05, Fig. 6E–H). Conversely, the elevated levels of BACE1 and PS1 in the hippocampus and cortex were attenuated by M-WYD compared to the Model group ($P < 0.01$ or 0.05, Fig. 6E–H). Although L-WYD and H-WYD demonstrated positive effects on certain Aβ-related enzymes, their effect was inferior to that of M-WYD (Fig. 6E–H). The experimental findings demonstrated that WYD effectively inhibited the Aβ production in the hippocampus and cortex of rats with CSD through the regulation of Aβ-related enzymes.

3.6. WYD reduces the inflammatory response in hippocampus and cortex of CSD rats via reducing the activated astrocytes and microglia

Neuroinflammation serves as another contributor to neuronal damage and synaptic dysfunction in central nervous system (CNS), and mounting evidence suggests that CSD may accelerate these pathological changes by triggering neuroinflammation (Camberos-Barraza et al., 2024; H. Gao et al., 2023; Zhao et al., 2023). As resident neurons in the brain, glial cells are closely associated with the occurrence of neuroinflammation. Astrocytes and microglia, the main types of immune inflammatory cells, are the sensitive factors in inflammatory response of the brain. Prior studies have elucidated the role of CSD in the activation of astrocytes and microglia, leading to the secretion of inflammatory cytokines (Misrani et al., 2024; Zhai et al., 2023). Astrocytes and microglia are respectively characterized by GFAP and IBA1. Consequently, we employed immunofluorescence to mark these proteins in the hippocampus and cortex, then measured the intensity of the fluorescence. The data depicted in Fig. 7A–D demonstrate a statistically significant elevation in the expression levels of GFAP and IBA1 within the hippocampal CA3 region and cortex of the Model group relative to the Control group ($P < 0.01$). In contrast, administration of M-WYD significantly attenuated the expression levels of GFAP and IBA1 in the hippocampal CA3 region and cortex of CSD rats compared to the Model group, consistent with our hypothesis ($P < 0.01$ or 0.05, Fig. 7A–D). No significant differences in GFAP and IBA1 expression were observed in the L-WYD and H-WYD groups ($P > 0.05$, Fig. 7A–D). The findings indicated that white CSD extract had the potential to suppress the activation of astrocytes and microglia. Furthermore, Western blot analysis was utilized to quantify the concentrations of IL-1β, IL-6, and TNF-α in the hippocampus and cortex. Significantly elevated levels of IL-1β, IL-6, and TNF-α were observed in the Model group compared to the Control group, and the administration of MYD resulted in a suppression of the expression of these pro-inflammatory cytokines, with the most pronounced effects observed in the M-WYD group ($P < 0.01$ or 0.05, Fig. 7E–H). These results suggested that WYD may attenuate the inflammatory response in the hippocampus and cortex of CSD rats through the suppression of astrocyte and microglia activation.

3.7. WYD suppresses NF-κB activity by activating the SIRT1/Nrf2 pathway in CSD rats

The SIRT1/Nrf2 pathway has been widely demonstrated to have an inhibitory effect on neuroinflammation and oxidative stress, and accumulated evidence suggests that activation of this pathway can alleviate neuronal damage, synaptic dysfunction and ferroptosis in CSD (J. Chen et al., 2023; Y. Li et al., 2023). To elucidate the molecular mechanisms underlying the protective effects of WYD in CSD model, the expression levels of SIRT1 and Nrf2 in the hippocampus and cortex were assessed via Western blot analysis. Relative to the Control group, the CSD induced a significant reduction in SIRT1 and Nrf2 protein levels in both the hippocampus and cortex of the Model group ($P < 0.01$, Fig. 8A–D). Nevertheless, administration of M-WYD effectively reversed the decline in SIRT1 and Nrf2 expression levels ($P < 0.01$ or 0.05, Fig. 8A–D). This

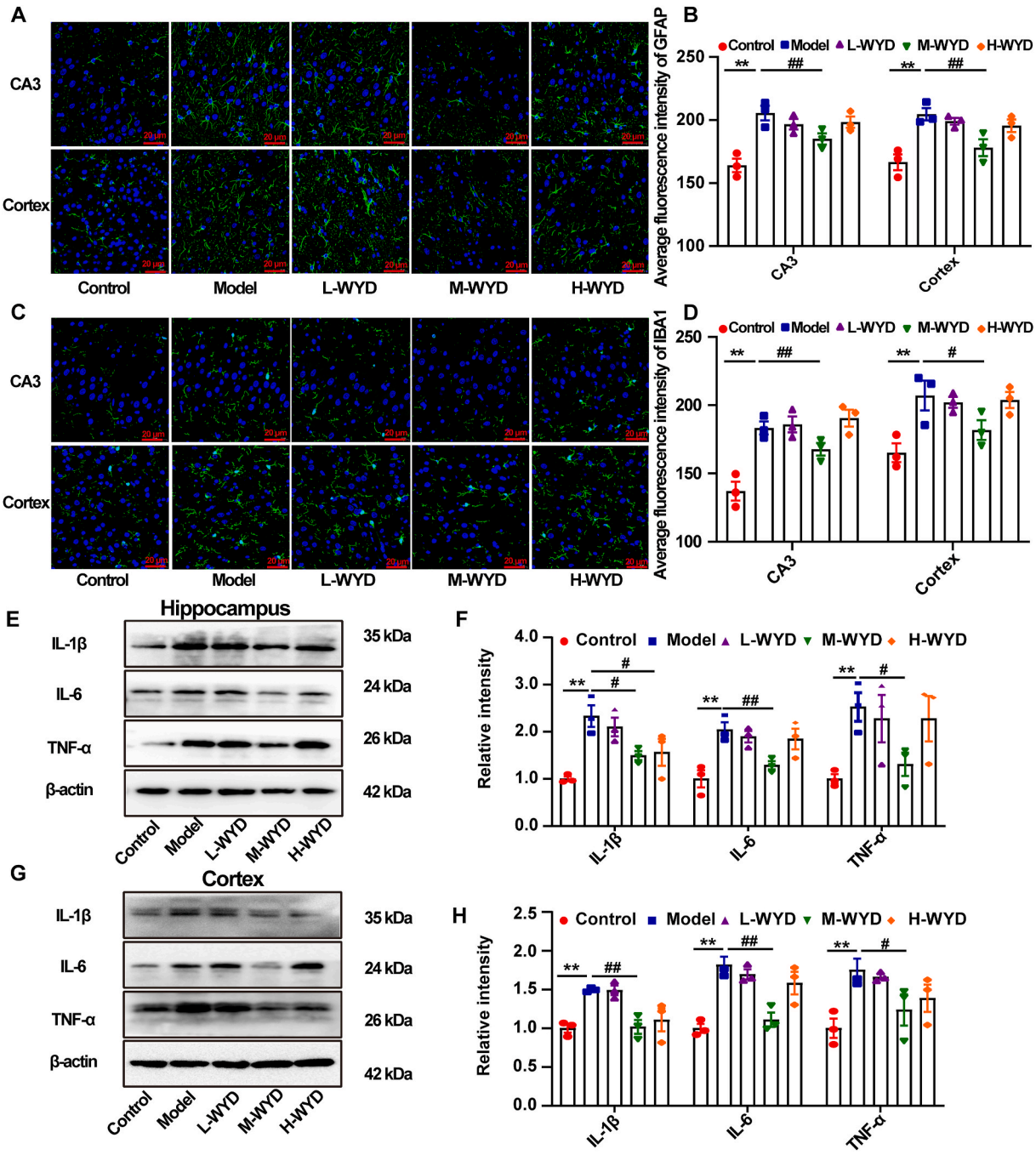

Fig. 7. WYD suppressed the activation of astrocytes and microglia, thus inhibiting the inflammatory response induced by CSD. (A) Immunofluorescence staining was conducted to detect GFAP in the hippocampal CA3 region and cortex, with a scale bar of 20 μm. (B) Fluorescence intensity of GFAP in hippocampal CA3 region and cortex (n = 3). (C) Immunofluorescence staining was performed to detect IBA1 in the hippocampal CA3 region and cortex, with a scale bar of 20 μm. (D) Fluorescence intensity of IBA1 in hippocampal CA3 region and cortex (n = 3). (E) The hippocampus demonstrated electrophoretic bands for IL-1β, IL-6, and TNF-α. (F) Hippocampus-specific quantitative analyses for IL-1β, IL-6, and TNF-α (n = 3). (G) The cortex demonstrated electrophoretic bands for IL-1β, IL-6, and TNF-α. (H) Cortex-specific quantitative analyses for IL-1β, IL-6, and TNF-α (n = 3).
Data are shown as mean ± SEM. **P < 0.01 compared to Control group; #P < 0.05 or ##P < 0.01 compared to Model group.

change was not observed in the L-WYD group, while H-WYD increased the protein expression levels of Nrf2 and SIRT1 ($P < 0.05$, Fig. 8A–D). Nevertheless, H-WYD is less effective compared to M-WYD, contrary to the Model group. NF-κB serves as a regulatory element within the SIRT1/Nrf2 signaling cascade. Activating the SIRT1/Nrf2 pathway can suppress NF-κB activity, leading to the inhibition of neuroinflammation (Y. J. Li et al., 2023). Accordingly, we examined the expression levels of factors associated with the NF-κB pathway, including IκBα, NF-κB p65, and their phosphorylated forms. Fig. 8A–D illustrated that CSD led to a notable rise in phosphorylated IκBα (Ser32) and phosphorylated NF-κB p65 (Ser536) levels in the hippocampus and cortex compared to the Control group ($P < 0.01$). Conversely, treatment with M-WYD significantly reduced the expression of these phosphorylated proteins ($P < 0.01$ or 0.05, Fig. 8A–D). However, L-WYD and H-WYD did not exhibit the similar effect as M-WYD, and we did not observe a noticeable decrease in these groups ($P > 0.05$, Fig. 8A–D). To sum up, the findings mentioned above showed that WYD could suppress NF-κB expression by activating the SIRT1/Nrf2 signaling pathway in CSD rats.

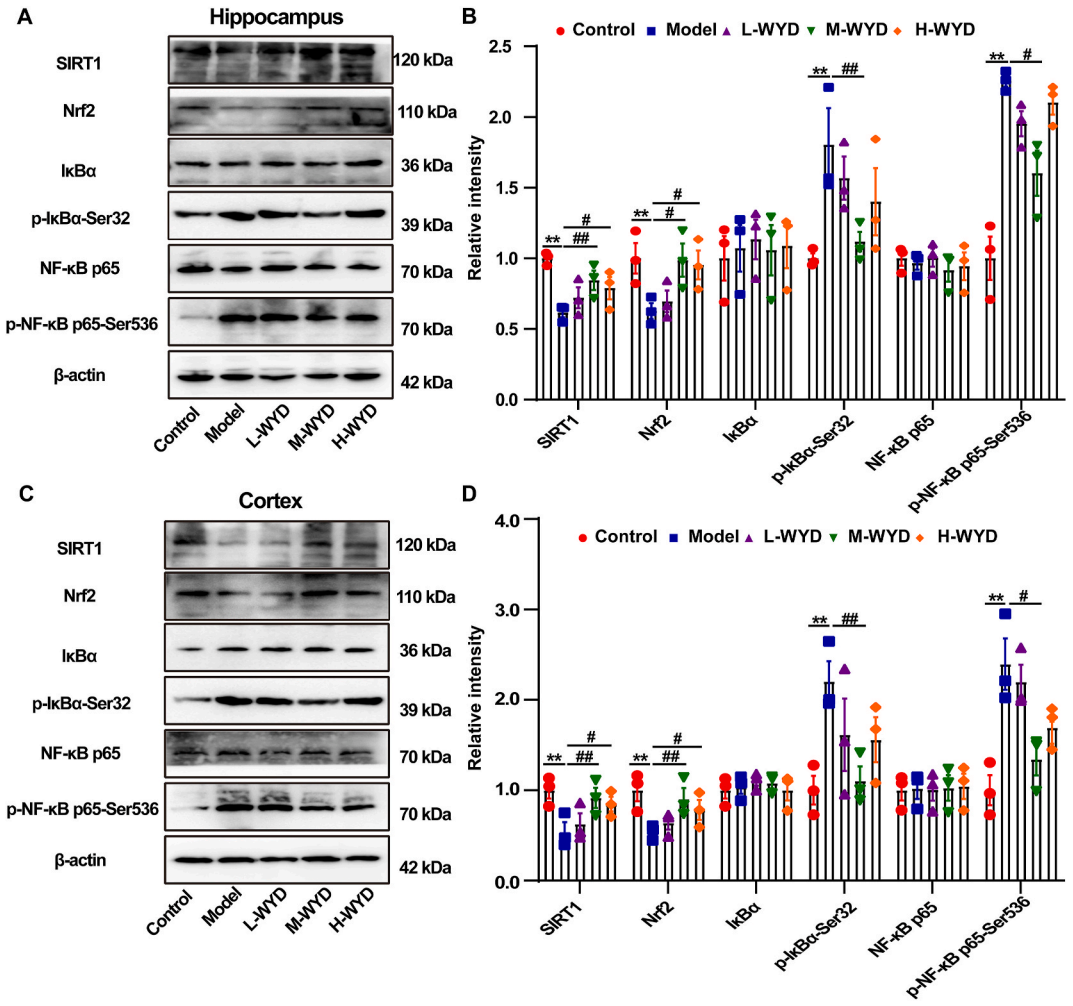

Fig. 8. Impact of WYD on the SIRT1/Nrf2/NF-κB pathway in rats with CSD. (A) The hippocampus demonstrated electrophoretic bands for SIRT1, Nrf2, IκBα, p-IκBα-Ser32, NF-κB p65 and p-NF-κB p65-Ser536. (B) Hippocampus-specific quantitative analyses for SIRT1, Nrf2, IκBα, p-IκBα-Ser32, NF-κB p65 and p-NF-κB p65-Ser536 (n = 3). (C) The cortex demonstrated electrophoretic bands for SIRT1, Nrf2, IκBα, p-IκBα-Ser32, NF-κB p65 and p-NF-κB p65-Ser536. (D) Cortex-specific quantitative analyses for SIRT1, Nrf2, IκBα, p-IκBα-Ser32, NF-κB p65 and p-NF-κB p65-Ser536 (n = 3).
Data are shown as mean ± SEM. **P < 0.01 compared to Control group; #P < 0.05 or ##P < 0.01 compared to Model group.

4. Discussion

The detrimental impact of sleep deprivation on cognitive function has been extensively researched, revealing substantial declines in memory, attention, and learning capacity (Salari et al., 2015, 2023). CSD not only results in immediate cognitive impairments but also elevates the risk of developing neurodegenerative disorders, such as AD (Kim et al., 2024). This association is primarily attributed to sleep's critical functions in clearing metabolic waste from the brain, consolidating memory, and facilitating neuronal repair (Shih et al., 2023). Therefore, sufficient sleep is crucial for the preservation of cognitive health.

Currently, nondrug interventions, especially the cognitive behavioral therapy, is considered an effective strategy to manage cognitive impairments-related to sleep disorders, and the effective therapeutic drugs are extremely limited (Morin and Jarrin, 2022). Chinese medicine clinical practitioners have confirmed that herbal formulas in the classical works have clinical efficacy in treating cognitive dysfunction-related to sleep disorders, of which WYD is the representative formulas. Furthermore, related clinical research has demonstrated that WYD can enhance cognitive function and sleep quality in patients suffering from insomnia (Tang, 2014). UHPLC-MS/MS analysis identified a variety of saponin compounds, flavonoid compounds, and organic acids in the WYD extract. Notably, ginsenosides such as Ginsenoside Rg1 and Ginsenoside Rg5 have demonstrated efficacy in ameliorating cognitive impairment and neuronal damage in sleep deprivation models through the modulation of energy metabolism and neuroinflammation (J. B. Chen et al., 2023; Jiang et al., 2024). Albiflorin and Ferulic acid confer neuroprotection by mitigating the production and accumulation of Aβpeptides (Ma et al., 2021; Singh et al., 2021). Furthermore, empirical studies have indicated that Gallic Acid, Chlorogenic Acid, and Kaempferol can mitigate synaptic dysfunction and neuronal loss in sleep deprivation models by attenuating neuroinflammation, enhancing immune function, and inhibiting oxidative stress (Du et al., 2023; Pang et al., 2023; Zhu et al., 2024). Therefore, in this study, we consciously selected WYD and investigated its mechanism of improving cognitive impairment and neuroprotection in CSD.

The present study utilized the MWM test to evaluate the effects of WYD on the cognitive abilities of CSD rats. Consistent with our hypothesis, WYD administration resulted in a reduced escape latency in CSD model rats. Compared to the Model group, the WYD-treated group exhibited a significantly higher number of platform crossings, an extended duration of time spent in the target quadrant, and a reduced swimming distance. These findings collectively suggest that WYD has the potential to ameliorate cognitive dysfunction in CSD rats.

Neurons and synapses are particularly important for maintaining

learning and memory. Accumulated evidence has confirmed that CSD can induce neuronal damage and synaptic dysfunction, leading to cognitive decline (N. Li et al., 2023; Vecsey et al., 2018; Zhang et al., 2024). To assess the neuroprotective impact of WYD on CSD, neurons in hippocampus and cortex were labeled by HE staining, Nissl staining and immunohistochemistry. HE and Nissl staining indicated that the administration of WYD reduced the pathological changes such as nuclear shrinkage and abnormal nuclei, while also boosting the neuron count in the hippocampus and cortex. Consistent with the results of Nissl staining, immunohistochemical analysis further confirmed the capacity of WYD to increase the presence of NeuN-positive neurons. These findings indicate that WYD may enhance the mitigation of pathological structural damage to neurons and neuronal loss caused by CSD. Synaptic dysfunction is another important pathological alteration of CSD model. Therefore, we employed Golgi-Cox staining and TEM to label and examine dendritic spines and synaptic ultrastructure in hippocampus and cortex, respectively. Golgi-Cox staining indicated that dendritic spines density and length in the hippocampus and cortex were enhanced by WYD. These dimensions of postsynaptic density (PSD), which is indicative of synaptic activity. As anticipated, the dimensions of PSD were enlarged by WYD in comparison to the Model group, aligning with our predictions. Moreover, Western blot analysis was employed to evaluate the expression levels of synaptic proteins, specifically PSD95 and SYN1, in the hippocampus and cortex. The findings revealed a significant upregulation of PSD95 and SYN1 proteins in the hippocampus and cortex of rats subjected to CSD. These findings imply that treatment with WYD exerts a neuroprotective effect on CSD model, potentially ameliorating neuronal damage and synaptic dysfunction.

Previous studies have demonstrated that high-quality sleep facilitates the clearance of Aβ, whereas both acute and chronic sleep restriction are associated with elevated levels of Aβ expression in the brain (Holth et al., 2019; Shokri-Kojori et al., 2018). Additionally, studies-related to AD have found that sleep deprivation can accelerate Aβ production and deposition (Duncan et al., 2022; Park et al., 2023). Aβ is recognized for its harmful effects on the brain, causing harm to neurons and synapses. Reducing Aβ expression in the brain has been shown to mitigate neuronal damage and synaptic dysfunction in sleep deprivation models (H. Gao et al., 2023; Liu et al., 2022). Immunofluorescence analysis was employed to investigate Aβ expression levels in the hippocampus and cortex, elucidating the mechanisms by which WYD treatment ameliorated these pathological changes in CSD rats. Furthermore, levels of $A\beta_{1\text{-}40}$ and $A\beta_{1\text{-}42}$ in the hippocampus and cortex were analyzed using ELISA kits. The experimental results indicate that WYD reduced Aβ production resulting from CSD and suppressed the expressions of $A\beta_{1\text{-}40}$ and $A\beta_{1\text{-}42}$. Previous studies have found that Aβ production or deposition is closely linked to Aβ-related enzymes (Li et al., 2020; M. Wang et al., 2023). Consequently, Western blot analysis was employed to assess the expression levels of ADAM10, BACE1, PS1, and IDE in the hippocampal and cortical regions. The administration of WYD was observed to elevate the levels of ADAM10 and IDE in the hippocampus and cortex of CSD rats, while concurrently reducing the expression of BACE1 and PS1. These findings suggest that WYD possesses the capacity to mitigate Aβ production in CSD by modulating Aβ-related enzymatic activity.

Neuroinflammation has been implicated as another contributing factor to pathological alterations, including neuronal apoptosis and synaptic dysfunction. The equilibrium between anti-inflammatory and pro-inflammatory processes is disrupted following CSD (Z. Wang et al., 2021; Xue et al., 2019). Astrocytes and microglia have been recognized as pivotal modulators of the inflammatory response in the brain. Previous studies have confirmed that activated astrocytes and microglia following sleep deprivation can stimulate the secretion of inflammatory molecules, resulting in heightened and worsened brain injury (L. Li et al., 2023; Manchanda et al., 2018). This research examined the impact of WYD on astrocytes and microglia by quantifying the levels of GFAP-positive astrocytes and IBA1-positive microglia. Significant activation of astrocytes and microglia in the hippocampal CA3 region and cortex was observed following CSD, with this activation being attenuated by WYD. Levels of IL-1β, IL-6, and TNF-α in the hippocampus and cortex were assessed via Western blot. The observed reduction in elevated levels of these cytokines following treatment with WYD supports the hypothesis that WYD may effectively mitigate neuroinflammation of CSD rats by modulating astrocyte and microglial activation.

Sirtunin 1 (SIRT1), a member of sirtunin family, regulates the neuroinflammation, ferroptosis and mitochondrial function of CNS diseases (Fang et al., 2021; Razick et al., 2023). Nuclear factor E2-related factor 2 (Nrf2) functions as an inhibitor of neuroinflammation, oxidative stress, and ferroptosis, which is regulated by SIRT1 (Bai et al., 2023; George et al., 2022). Existing research has demonstrated that the SIRT1/Nrf2 pathway is suppressed following CSD, whereas activation of this pathway has been shown to ameliorate neuronal damage, synaptic dysfunction, ferroptosis, and mitochondrial dysfunction induced by CSD (Wei et al., 2024; Yang et al., 2022). To delve deeper into the molecular mechanism of WYD's neuroprotective effects on CSD model rats, we conducted an analysis of SIRT1 and Nrf2 expression levels in the hippocampus and cortex. Consistent with previous literatures, the level of SIRT1 and Nrf2 in the hippocampus and cortex were significantly reduced following CSD, with WYD boosting their expression. This result confirmed that WYD could activate SIRT1/Nrf2 pathway in CSD model rats. Nuclear factor-kappa B (NF-κB), a significant downstream mediator of Nrf2, and has been shown to release proinflammatory factors, leading to impaired neural plasticity in CNS diseases (J. Chen et al., 2023; Y. Li et al., 2023). Moreover, mounting proof suggests that the NF-κB pathway can be suppressed through the activation of Nrf2, leading to enhanced protection against neuronal damage and neuroinflammation (Nakano-Kobayashi et al., 2023; Wu et al., 2022). Consequently, we conducted an examination of protein levels associated with NF-κB pathway, specifically IκBα, NF-κB p65, and their phosphorylated variants. Our experimental results indicate that WYD treatment led to a reduction in phosphorylated IκBα-Ser32 and phosphorylated NF-κB p65-Ser536 levels in the hippocampus and cortex of CSD rats, while having no significant effect on IκBα and NF-κB p65. Collectively, the cumulative results of the experiments indicated that possesses the capacity to inhibit NF-κB expression through the activation of the SIRT1/Nrf2 pathway in rats with CSD.

5. Conclusion

Overall, this study demonstrated WYD could protect against neuronal damage, synaptic issues, Aβ production, and neuroinflammation in CSD model rats by influencing Aβ-related enzymes and the SIRT1/Nrf2/NF-κB pathway. Consequently, WYD holds potential as a preventive agent against cognitive impairment associated with sleep disorders. However, the scope of our current research is limited, necessitating further investigations to elucidate the precise molecular mechanisms by which WYD ameliorates cognitive deficits linked to sleep disturbances.

CRediT authorship contribution statement

Zhengyu Wang: Writing – original draft, Methodology, Formal analysis. **Dan Wu:** Writing – original draft, Methodology. **Xinyi Hu:** Writing – original draft, Investigation, Conceptualization. **Xuan Hu:** Methodology, Investigation, Conceptualization. **Qihang Zhu:** Supervision, Investigation, Data curation. **Bixuan Lai:** Validation, Project administration, Formal analysis. **Chuhua Zeng:** Writing – review & editing, Validation, Supervision. **Qinghua Long:** Writing – review & editing, Supervision, Project administration.

Ethics approval

In accordance with local legislation and institutional requirements, the study was censored and approved by the Health Ethics Committee of Hubei Minzu University (authorization number: 202382).

Declaration of competing interest

The authors assert that the research was carried out without any commercial or financial affiliations that could be perceived as a possible conflict of interest.

Acknowledgements

This study was funded by the National Natural Science Foundation of China (Grant No. 82204964), the Hubei Provincial College Students' Innovation and Entrepreneurship Training Project (Grant No. S202310517024), and open fund project of Hubei Provincial Key Laboratory of Occurrence and Intervention of Rheumatic Disease (Grant No. PT022307).

Appendix A. Supplementary data

Supplementary data to this article can be found online at https://doi.org/10.1016/j.jep.2024.118939.

Data availability

If further information is required, the original data will be provided on request. Further inquiries should be directed to the corresponding author.

References

Bai, X., Bian, Z., Zhang, M., 2023. Targeting the Nrf2 signaling pathway using phytochemical ingredients: a novel therapeutic road map to combat neurodegenerative diseases. Phytomedicine. https://doi.org/10.1016/j.phymed.2022.154582.

Beiyu, Z., Rong, Z., Yi, Z., Shan, W., Peng, L., Meng, W., Wei, P., Ye, Y., Qiumin, Q., 2024. Oxidative stress is associated with Aβ accumulation in chronic sleep deprivation model. Brain Res. 1829. https://doi.org/10.1016/j.brainres.2024.148776.

Bellesi, M., Vivo, L. De, Chini, M., Gilli, F., Tononi, G., Cirelli, C., 2017. Sleep loss promotes astrocytic phagocytosis and microglial activation in mouse cerebral cortex. J. Neurosci. 37. https://doi.org/10.1523/JNEUROSCI.3981-16.2017.

Camberos-Barraza, J., Camacho-Zamora, A., Bátiz-Beltrán, J.C., Osuna-Ramos, J.F., Rábago-Monzón, Á.R., Valdez-Flores, M.A., Angulo-Rojo, C.E., Guadrón-Llanos, A. M., Picos-Cárdenas, V.J., Calderón-Zamora, L., Norzagaray-Valenzuela, C.D., Cárdenas-Torres, F.I., De la Herrán-Arita, A.K., 2024. Sleep, glial function, and the endocannabinoid system: implications for neuroinflammation and sleep disorders. Int. J. Mol. Sci. https://doi.org/10.3390/ijms25063160.

Cao, Y., Li, Qinglin, Liu, L., Wu, H., Huang, F., Wang, C., Lan, Y., Zheng, F., Xing, F., Zhou, Q., Li, Qi, Shi, H., Zhang, B., Wang, Z., Wu, X., 2019. Modafinil protects hippocampal neurons by suppressing excessive autophagy and apoptosis in mice with sleep deprivation. Br. J. Pharmacol. 176. https://doi.org/10.1111/bph.14626.

Chen, J., Xiao, L., Chen, Y., Li, W., Liu, Y., Zhou, Y., Tan, H., 2023. YT521-B homology domain containing 1 ameliorates mitochondrial damage and ferroptosis in sleep deprivation by activating the sirtuin 1/nuclear factor erythroid-derived 2-like 2/heme oxygenase 1 pathway. Brain Res. Bull. 197. https://doi.org/10.1016/j.brainresbull.2023.03.008.

Chen, L., Huang, J., Yang, L., Zeng, X.A., Zhang, Ya, Wang, X., Chen, M., Li, X., Zhang, Yifan, Zhang, M., 2017. Sleep deprivation accelerates the progression of alzheimer's disease by influencing Aβ-related metabolism. Neurosci. Lett. 650. https://doi.org/10.1016/j.neulet.2017.04.047.

Dopheide, J.A., 2020. Insomnia overview: epidemiology, pathophysiology, diagnosis and monitoring, and nonpharmacologic therapy. Am. J. Manag. Care. https://doi.org/10.37765/AJMC.2020.42769.

Du, Y.Y., Sun, T., Yang, Q., Liu, Q.Q., Li, J.M., Yang, L., Luo, L.X., 2023. Therapeutic potential of Kaempferol against sleep deprivation-induced cognitive impairment: modulation of neuroinflammation and synaptic plasticity disruption in mice. ACS Pharmacol. Transl. Sci. 6. https://doi.org/10.1021/acsptsci.3c00226.

Duncan, M.J., Guerriero, L.E., Kohler, K., Beechem, L.E., Gillis, B.D., Salisbury, F., Wessel, C., Wang, J., Sunderam, S., Bachstetter, A.D., O'Hara, B.F., Murphy, M.P., 2022. Chronic fragmentation of the daily sleep-wake rhythm increases amyloid-beta levels and neuroinflammation in the 3xTg-AD mouse model of alzheimer's disease. Neuroscience 481. https://doi.org/10.1016/j.neuroscience.2021.11.042.

Fang, Y., Wang, X., Yang, D., Lu, Y., Wei, G., Yu, W., Liu, X., Zheng, Q., Ying, J., Hua, F., 2021. Relieving cellular energy stress in aging, neurodegenerative, and metabolic diseases, SIRT1 as a therapeutic and promising node. Front. Aging Neurosci. https://doi.org/10.3389/fnagi.2021.738686.

Gao, H., Zhang, Y., Luo, D., Xu, J., Tan, S., Li, Y., Qi, W., Zhai, Q., Wang, Q., 2023. Activation of the hippocampal DRD2 alleviates neuroinflammation, synaptic plasticity damage and cognitive impairment after sleep deprivation. Mol. Neurobiol. 60. https://doi.org/10.1007/s12035-023-03514-5.

George, M., Tharakan, M., Culberson, J., Reddy, A.P., Reddy, P.H., 2022. Role of Nrf2 in aging, Alzheimer's and other neurodegenerative diseases. Ageing Res. Rev. https://doi.org/10.1016/j.arr.2022.101756.

Hao, Y., Shao, L., Hou, J., Zhang, Y., Ma, Y., Liu, J., Xu, C., Chen, F., Cao, L.H., Ping, Y., 2023. Resveratrol and Sir2 reverse sleep and memory defects induced by amyloid precursor protein. Neurosci. Bull. 39. https://doi.org/10.1007/s12264-023-01056-3.

Holth, J.K., Fritschi, S.K., Wang, C., Pedersen, N.P., Cirrito, J.R., Mahan, T.E., Finn, M.B., Manis, M., Geerling, J.C., Fuller, P.M., Lucey, B.P., Holtzman, D.M., 2019. The sleep-wake cycle regulates brain interstitial fluid tau in mice and CSF tau in humans. Science 363. https://doi.org/10.1126/science.aav2546.

Jiang, N., Yao, C., Zhang, Y., Sun, X., Choudhary, M.I., Liu, X., 2024. Ginsenoside Rg1 attenuates chronic sleep deprivation-induced hippocampal mitochondrial dysfunction and improves memory by the AMPK-SIRT3 pathway. J. Agric. Food Chem. 72. https://doi.org/10.1021/acs.jafc.3c04618.

Kang, Z., Lin, Y., Su, C., Li, S., Xie, W., Wu, X., 2023. Hsp70 ameliorates sleep deprivation-induced anxiety-like behavior and cognitive impairment in mice. Brain Res. Bull. 204. https://doi.org/10.1016/j.brainresbull.2023.110791.

Kim, D.Y., Kim, S.-M., Han, I.-O., 2024. Chronic rapid eye movement sleep deprivation aggravates the pathogenesis of Alzheimer's disease by decreasing brain O-GlcNAc cycling in mice. J. Neuroinflammation 21, 180. https://doi.org/10.1186/s12974-024-03179-4.

Li, G., Qin, Z., 2019. Experimental study of the effect of WuYou Decoction on the expressions of hippocampal 5-HT1AR and 5-HT2AR in depression model rats. World Journal of Integrated Traditional and Western Medicine 14, 1099–1104. https://doi.org/10.13935/j.cnki.sjzx.190816.

Li, J.M., Huang, A.X., Yang, L., Li, P., Gao, W., 2023. A sensitive LC-MS/MS method-based pharmacokinetic study of fifteen active ingredients of Yindan Xinnaotong soft capsule in rats and its potential mechanism in the treatment of cardiovascular diseases. J. Chromatogr., B: Anal. Technol. Biomed. Life Sci. 1220. https://doi.org/10.1016/j.jchromb.2023.123663.

Li, Y., Zhang, J., Wan, J., Liu, A., Sun, J., 2020. Melatonin regulates Aβ production/clearance balance and Aβ neurotoxicity: a potential therapeutic molecule for Alzheimer's disease. Biomed. Pharmacother. https://doi.org/10.1016/j.biopha.2020.110887.

Li, Z.H., Cheng, L., Wen, C., Ding, L., You, Q.Y., Zhang, S.B., 2022. Activation of CNR1/PI3K/AKT pathway by tanshinone IIA protects hippocampal neurons and ameliorates sleep deprivation-induced cognitive dysfunction in rats. Front. Pharmacol. 13. https://doi.org/10.3389/fphar.2022.823732.

Liu, S., Lei, Q., Liu, Y., Zhang, X., Li, Z., 2022. Acoustic stimulation improves memory and reverses the contribution of chronic sleep deprivation to pathology in 3xTgAD mice. Brain Sci. 12. https://doi.org/10.3390/brainsci12111509.

Long, Q., Li, T., Zhu, Q., He, L., Zhao, B., 2024. SuanZaoRen decoction alleviates neuronal loss, synaptic damage and ferroptosis of AD via activating DJ-1/Nrf2 signaling pathway. J. Ethnopharmacol. 323. https://doi.org/10.1016/j.jep.2023.117679.

Long, Q.H., Wu, Y.G., He, L.L., Ding, L., Tan, A.H., Shi, H.Y., Wang, P., 2021. Suan-Zao-Ren Decoction ameliorates synaptic plasticity through inhibition of the Aβ deposition and JAK2/STAT3 signaling pathway in AD model of APP/PS1 transgenic mice. Chin. Med. 16. https://doi.org/10.1186/s13020-021-00425-2.

Lu, C., Lv, J., Jiang, N., Wang, H., Huang, H., Zhang, L., Li, S., Zhang, N., Fan, B., Liu, X., Wang, F., 2020. Protective effects of Genistein on the cognitive deficits induced by chronic sleep deprivation. Phytother Res. 34. https://doi.org/10.1002/ptr.6567.

Lyons, L.C., Vanrobaeys, Y., Abel, T., 2023. Sleep and memory: the impact of sleep deprivation on transcription, translational control, and protein synthesis in the brain. J. Neurochem. https://doi.org/10.1111/jnc.15787.

Ma, X., Song, M., Yan, Y., Ren, G., Hou, J., Qin, G., Wang, W., Li, Z., 2021. Albiflorin alleviates cognitive dysfunction in STZ-induced rats. Aging 13. https://doi.org/10.18632/aging.203274.

Manchanda, S., Singh, H., Kaur, T., Kaur, G., 2018. Low-grade neuroinflammation due to chronic sleep deprivation results in anxiety and learning and memory impairments. Mol. Cell. Biochem. 449. https://doi.org/10.1007/s11010-018-3343-7.

Misrani, A., Tabassum, S., Zhang, Z.Y., Tan, S.H., Long, C., 2024. Urolithin A prevents sleep-deprivation-induced neuroinflammation and mitochondrial dysfunction in young and aged mice. Mol. Neurobiol. 61. https://doi.org/10.1007/s12035-023-03651-x.

Morin, C.M., Jarrin, D.C., 2022. Epidemiology of insomnia: prevalence, course, risk factors, and public health burden. Sleep Med Clin. https://doi.org/10.1016/j.jsmc.2022.03.003.

Nakano-Kobayashi, A., Canela, A., Yoshihara, T., Hagiwara, M., 2023. Astrocyte-targeting therapy rescues cognitive impairment caused by neuroinflammation via the Nrf2 pathway. Proc. Natl. Acad. Sci. U. S. A. 120. https://doi.org/10.1073/pnas.2303809120.

Niu, L., Zhang, F., Xu, X., Yang, Y., Li, S., Liu, H., Le, W., 2022. Chronic sleep deprivation altered the expression of circadian clock genes and aggravated Alzheimer's disease neuropathology. Brain Pathol. 32. https://doi.org/10.1111/bpa.13028.

Pang, X., Xu, Y., Xie, S., Zhang, T., Cong, L., Qi, Y., Liu, L., Li, Q., Mo, M., Wang, G., Du, X., Shen, H., Li, Y., 2023. Gallic acid ameliorates cognitive impairment caused by

sleep deprivation through antioxidant effect. Exp Neurobiol 32. https://doi.org/10.5607/en23015.
Parhizkar, S., Gent, G., Chen, Y., Rensing, N., Gratuze, M., Strout, G., Sviben, S., Tycksen, E., Zhang, Q., Gilmore, P.E., Sprung, R., Malone, J., Chen, W., Serrano, J.R., Bao, X., Lee, C., Wang, C., Landsness, E., Fitzpatrick, J., Wong, M., Townsend, R., Colonna, M., Schmidt, R.E., Holtzman, D.M., 2023. Sleep deprivation exacerbates microglial reactivity and Aβ deposition in a TREM2-dependent manner in mice. Sci. Transl. Med. 15. https://doi.org/10.1126/scitranslmed.ade6285.
Park, J., Kim, D.Y., Hwang, G.S., Han, I.O., 2023. Repeated sleep deprivation decreases the flux into hexosamine biosynthetic pathway/O-GlcNAc cycling and aggravates Alzheimer's disease neuropathology in adult zebrafish. J. Neuroinflammation 20. https://doi.org/10.1186/s12974-023-02944-1.
Paul, S., Vidusha, K., Thilagar, S., Lakshmanan, D.K., Ravichandran, G., Arunachalam, A., 2022. Advancement in the contemporary clinical diagnosis and treatment strategies of insomnia disorder. Sleep Med. https://doi.org/10.1016/j.sleep.2022.02.018.
Qin, Z., Wu, S.D., Wang, Z., 2014. Experimental study on the behavior of CUMS model rats treated with WuYou Decoction. Liaoning J Tradit Chin Med 41, 1036–1039. https://doi.org/10.13192/j.issn.1000-1719.2014.05.089.
Razick, D.I., Akhtar, M., Wen, J., Alam, M., Dean, N., Karabala, M., Ansari, U., Ansari, Z., Tabaie, E., Siddiqui, S., 2023. The role of sirtuin 1 (SIRT1) in neurodegeneration. Cureus. https://doi.org/10.7759/cureus.40463.
Salari, M., Esmaeilpour, K., Mohammadipoor-Ghasemabad, L., Taheri, F., Hosseini, M., Sheibani, V., 2023. Impact of sleep deprivation on the brain's inflammatory response triggered by lipopolysaccharide and its consequences on spatial learning and memory and long-term potentiation in male rats. Neuroimmunomodulation 31. https://doi.org/10.1159/000535784.
Salari, M., Sheibani, V., Saadati, H., Pourrahimi, A., khaksarihadad, M., Esmaeelpour, K., Khodamoradi, M., 2015. The compensatory effect of regular exercise on long-term memory impairment in sleep deprived female rats. Behav. Process. 119. https://doi.org/10.1016/j.beproc.2015.06.014.
Shih, N.C., Barisano, G., Lincoln, K.D., Mack, W.J., Sepehrband, F., Choupan, J., 2023. Effects of sleep on brain perivascular space in a cognitively healthy population. Sleep Med. 111. https://doi.org/10.1016/j.sleep.2023.09.024.
Shokri-Kojori, E., Wang, G.J., Wiers, C.E., Demiral, S.B., Guo, M., Kim, S.W., Lindgren, E., Ramirez, V., Zehra, A., Freeman, C., Miller, G., Manza, P., Srivastava, T., De Santi, S., Tomasi, D., Benveniste, H., Volkow, N.D., 2018. β-Amyloid accumulation in the human brain after one night of sleep deprivation. Proc. Natl. Acad. Sci. U. S. A. 115. https://doi.org/10.1073/pnas.1721694115.
Singh, Y.P., Rai, H., Singh, G., Singh, G.K., Mishra, S., Kumar, S., Srikrishna, S., Modi, G., 2021. A review on ferulic acid and analogs based scaffolds for the management of Alzheimer's disease. Eur. J. Med. Chem. https://doi.org/10.1016/j.ejmech.2021.113278.
Tang, J., 2014. WuYou Decoction improved sleep quality and cognitive function in 32 patients with insomnia. Practical Clin. J. Integrated Tradit. Chin. West. Med. 14, 84–85. https://doi.org/10.13638/j.issn.1671-4040.2014.05.060.
Vecsey, C.G., Huang, T., Abel, T., 2018. Sleep deprivation impairs synaptic tagging in mouse hippocampal slices. Neurobiol. Learn. Mem. 154. https://doi.org/10.1016/j.nlm.2018.03.016.
Wadhwa, M., Prabhakar, A., Ray, K., Roy, K., Kumari, P., Jha, P.K., Kishore, K., Kumar, S., Panjwani, U., 2017. Inhibiting the microglia activation improves the spatial memory and adult neurogenesis in rat hippocampus during 48h of sleep deprivation. J. Neuroinflammation 14. https://doi.org/10.1186/s12974-017-0998-z.
Wang, C., Gao, W.-R., Yin, J., Wang, Z.-J., Qi, J.-S., Cai, H.-Y., Wu, M.-N., 2021. Chronic sleep deprivation exacerbates cognitive and synaptic plasticity impairments in APP/PS1 transgenic mice. Behav. Brain Res. 412, 113400. https://doi.org/10.1016/j.bbr.2021.113400.
Wang, H., Huang, H., Jiang, N., Zhang, Y., Lv, J., Liu, X., 2022. Tenuifolin ameliorates chronic restraint stress-induced cognitive impairment in C57BL/6J mice. Phytother Res. 36. https://doi.org/10.1002/ptr.7402.
Wang, M., Zhao, H., Zhang, Z., Zhao, Z., Wu, H., 2023. Down-regulating insulin-like growth factor-1 receptor reduces amyloid-β deposition in mice cortex induced by chronic sleep restriction. Neurosci. Lett. 808. https://doi.org/10.1016/j.neulet.2023.137189.
Wei, R.M., Zhang, Y.M., Zhang, K.X., Liu, G.X., Li, X.Y., Zhang, J.Y., Lun, W.Z., Liu, X.C., Chen, G.H., 2024. An enriched environment ameliorates maternal sleep deprivation-induced cognitive impairment in aged mice by improving mitochondrial function via the Sirt1/PGC-1α pathway. Aging 16. https://doi.org/10.18632/aging.205385.
Wu, S., Liao, X., Zhu, Z., Huang, R., Chen, M., Huang, A., Zhang, J., Wu, Q., Wang, J., Ding, Y., 2022. Antioxidant and anti-inflammation effects of dietary phytochemicals: the Nrf2/NF-κB signalling pathway and upstream factors of Nrf2. Phytochemistry. https://doi.org/10.1016/j.phytochem.2022.113429.
Xiong, Y., Tvedt, J., Åkerstedt, T., Cadar, D., Wang, H.X., 2024. Impact of sleep duration and sleep disturbances on the incidence of dementia and Alzheimer's disease: a 10-year follow-up study. Psychiatr. Res. 333. https://doi.org/10.1016/j.psychres.2024.115760.
Xue, R., Wan, Y., Sun, X., Zhang, X., Gao, W., Wu, W., 2019. Nicotinic mitigation of neuroinflammation and oxidative stress after chronic sleep deprivation. Front. Immunol. 10. https://doi.org/10.3389/fimmu.2019.02546.
Yang, Y., Wang, X., Xiao, A., Han, J., Wang, Z., Wen, M., 2022. Ketogenic diet prevents chronic sleep deprivation-induced Alzheimer's disease by inhibiting iron dyshomeostasis and promoting repair via Sirt1/Nrf2 pathway. Front. Aging Neurosci. 14. https://doi.org/10.3389/fnagi.2022.998292.
Ye, H. Tian, Lu, C. Qiang, Wang, C., Zhang, D., Li, Y. Fei, Feng, X. Yun, Wang, H. Peng, Mao, Yuan, Y., Ji, huo, M., Yang, J., 2023. Plasma Aβ level alterations after sleep deprivation correspond to brain structural remodeling in medical night shift workers. Brain Res. Bull. 203. https://doi.org/10.1016/j.brainresbull.2023.110776.
Zhai, Q., Zhang, Y., Ye, M., Zhu, S., Sun, J., Wang, Y., Deng, B., Ma, D., Wang, Q., 2023. Reducing complement activation during sleep deprivation yields cognitive improvement by dexmedetomidine. Br. J. Anaesth. 131. https://doi.org/10.1016/j.bja.2023.04.044.
Zhang, Y.M., Wei, R.M., Feng, Y.Z., Zhang, K.X., Ge, Y.J., Kong, X.Y., Li, X.Y., Chen, G.H., 2024. Sleep deprivation aggravates lipopolysaccharide-induced anxiety, depression and cognitive impairment: the role of pro-inflammatory cytokines and synaptic plasticity-associated proteins. J. Neuroimmunol. 386. https://doi.org/10.1016/j.jneuroim.2023.578252.
Zhang, Y.M., Wei, R.M., Ni, M.Z., Wu, Q.T., Li, Y., Ge, Y.J., Kong, X.Y., Li, X.Y., Chen, G.H., 2023. An enriched environment improves maternal sleep deprivation-induced cognitive deficits and synaptic plasticity via hippocampal histone acetylation. Brain Behav 13. https://doi.org/10.1002/brb3.3018.
Zhao, B., Liu, P., Wei, M., Li, Y., Liu, J., Ma, L., Shang, S., Jiang, Y., Huo, K., Wang, J., Qu, Q., 2019. Chronic sleep restriction induces Aβ accumulation by disrupting the balance of Aβ production and clearance in rats. Neurochem. Res. 44. https://doi.org/10.1007/s11064-019-02719-2.
Zhao, B., Wei, D., Long, Q., Chen, Q., Wang, F., Chen, L., Li, Z., Li, T., Ma, T., Liu, W., Wang, L., Yang, C., Zhang, X., Wang, P., Zhang, Z., 2024. Altered synaptic currents, mitophagy, mitochondrial dynamics in Alzheimer's disease models and therapeutic potential of Dengzhan Shengmai capsules intervention. J Pharm Anal 14, 348–370. https://doi.org/10.1016/j.jpha.2023.10.006.
Zhao, N., Chen, Q.G., Chen, X., Liu, X.T., Geng, F., Zhu, M.M., Yan, F.L., Zhang, Z.J., Ren, Q.G., 2023. Intestinal dysbiosis mediates cognitive impairment via the intestine and brain NLRP3 inflammasome activation in chronic sleep deprivation. Brain Behav. Immun. 108. https://doi.org/10.1016/j.bbi.2022.11.013.
Zhu, H., Shen, F., Wang, X., Qian, H., Liu, Y., 2024. Chlorogenic acid improves the cognitive deficits of sleep-deprived mice via regulation of immunity function and intestinal flora. Phytomedicine 123. https://doi.org/10.1016/j.phymed.2023.155194.
Zielinski, M.R., Kim, Y., Karpova, S.A., McCarley, R.W., Strecker, R.E., Gerashchenko, D., 2014. Chronic sleep restriction elevates brain interleukin-1 beta and tumor necrosis factor-alpha and attenuates brain-derived neurotrophic factor expression. Neurosci. Lett. 580. https://doi.org/10.1016/j.neulet.2014.07.043.